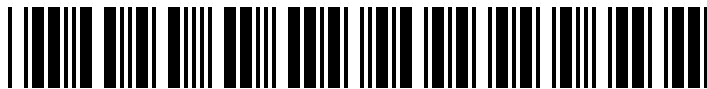


ECMM102

Group Project (Meng) (A, TRM1+2 2017/8)

049728

1029797



650019887

Coursework: Individual contribution to the group achievement**Submission Deadline:** Mon 14th May 2018 12:00**Personal tutor:** Dr Khurram Wadee**Marker name:** Tabor**Word count:** 15206

By submitting coursework you declare that you understand and consent to the University policies regarding plagiarism and mitigation (these can be seen online at www.exeter.ac.uk/plagiarism, and www.exeter.ac.uk/mitigation respectively), and that you have read your school's rules for submission of written coursework, for example rules on maximum and minimum number of words. Indicative/first marks are provisional only.

First marker's comments

Indicative
mark

Second marker's comments

Second mark

Moderator's comments

Agreed mark



I2 Report

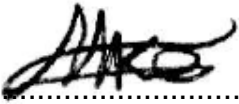
Determination of a Viscosity Model for an Olive Stone Powder and
Water Suspension for Primary Sedimentation Tank Modelling

Michael-Manuel Mendoza-Bollam

2018

4th year MEng Group Project

I certify that all material in this thesis that is not my own work has been identified and that no material has been included for which a degree has previously been conferred on me.

Signed.....

College of Engineering, Mathematics, and Physical Sciences
University of Exeter

I2 Report

ECMM102

Title:

Word count: 15206

Number of pages: 40

Date of submission: Monday, 14 May 2018

Student Name: Michael-Manuel Mendoza-Bollam

Programme: MENG Mechanical Engineering

Student number: 650019887

Candidate number: 049728

Supervisor: Prof Gavin Tabor

Abstract

This report aimed to identify and test the practical suitability of a viscosity model for an olive stone powder and water suspension, which is normally used in the water treatment industry as an experimental wastewater substitute. This was done to support the validation of an OpenFOAM[®] CFD model on two sedimentation tanks through empirical experiments conducted in the University of Exeter Fluids Lab. Focus was placed on characterising the olive stone powder, purchased from Goonvean Fibres[®], to determine the proper viscosity model. The size distribution, average aspect ratio and random close-packing fraction of the particles were determined. Rheological studies with several particle concentrations was performed with water as the suspending medium. Several suspension viscosity models were fitted to the data from this study using regression analysis. The model providing the best rheological behaviour prediction was then programmed into the OpenFOAM[®] software.

Most of the powder particles were between the sizes of 125 μ m and 32 μ m. The average aspect ratio was found to be 1.52 ± 0.04 , indicating that the particles are prolate in shape. The random close-packing fraction of the particles was 0.46 ± 0.07 . The rheological studies showed that the olive stone powder and water suspension is rapidly settling, time-dependent, shear thinning and Non-Newtonian at high concentrations. The viscosity model chosen to predict the behaviour of the suspension was the one proposed by S. Mueller^[32], because it considers the Non-Newtonian behaviour of the suspension at high concentrations. This theoretically should have provided better modelling of the olive stone suspension when implemented in the OpenFOAM[®] CFD software. However, when implemented it was found to be non-viable in practice, with the computational framework used in this work, due to unacceptably long computational times. This made the Muller model computationally expensive when compared to other Newtonian suspension models analysed in this work.

Keywords: Rheology, Relative Apparent Viscosity, OpenFOAM[®], Olive Stone Powder

Acknowledgments

I would like to thank the project supervisor Prof Gavin Tabor for his support and guidance throughout the project. Shenan Grossberg, Dr Joana Zaragoza, Angela Elliot, Dr Yat-Tarn Shyng, Julian Yates, Siobhan Kelley, Dr. Hong Chang and my mother and father for their kindness, patience and willingness to help and share their knowledge. I could not have finished this report without them.

Table of Contents

1. Introduction and Background	1
1.1. Waste Water Treatment and Sewage Sludge.....	2
1.2. Properties of Primary Sludge and Olive Stone Powder	2
1.3. Experimental Work	3
1.4. CFD Simulation	3
1.5. Project Objectives and Deliverables	4
2. Literature Review	5
3. Theoretical Background and Experimental Work	9
3.1. Governing Equations	9
3.1.1. Newtonian and Non-Newtonian Fluids.....	9
3.1.2. Suspension Rheology and Factors That Affect It.....	11
3.1.3. Suspension Viscosity Models	14
3.2. Experimental Work	15
3.2.1. Particle Size Distribution of Olive Stone Powder	15
3.2.2. Average Particle Geometry of Olive Stone Powder.....	17
3.2.3. Random Close-Packing Fraction of Olive Stone Powder	18
3.2.4. Rheology of an Olive Stone Suspension	19
3.3. CFD Simulations and OpenFOAM® Programming	20
3.3.1. Introducing a New Viscosity Model	22
3.4. Results Analysis	23
4. Presentation of Experimental and CFD Results.....	24
4.1. Particle Size Distribution of Olive Stone Powder	24
4.2. Average Particle Geometry of Olive Stone Powder	26
4.3. Random Close-Packing Fraction of Olive Stone Powder	27
4.4. Rheology of an Olive Stone Suspension.....	28
4.5. OpenFOAM® CFD Simulations	32
4.5.1. Modified ARMFELD Rectangular Sedimentation Tank	32
4.5.2. Swirl-Flo® Sedimentation Tank	33
5. Discussion and Conclusions	34
5.1. Discussion.....	34
5.2. Conclusions	35
5.3. Further Work	36
6. Project Management.....	36
6.1. Project and Time Management.....	36
6.2. Budget	37
6.3. Sustainability and Health and Safety	37
7. Contribution to Group Functioning.....	38
8. References.....	38

1. Introduction and Background

Sewage, or *urban waste water*, is defined in the European Union (EU) Directive *The Urban Waste Water Treatment Directive* ^[1]. Within this Directive, urban waste water is described as “*the mixture of domestic waste water from kitchens, bathrooms and toilets, the waste water from industries discharging to sewers and rainwater run-off from roads and other impermeable surfaces such as roofs, pavements and roads draining to sewers*” ^{[1][2]}.

Computer models are of increasing value in the optimisation procedure of sewage treatment as they are cost-effective to run since they obviate the need to carry out expensive laboratory tests on actual sewage.

The work documented in this report was done as part of a wider-ranging group project undertaken to create an experimentally validated Computational Fluid Dynamics (CFD) simulation of two different sewage sedimentation tanks. The tanks were a Hydrodynamic Vortex Separator (HDVS) Swirl-Flo[®] and a modified ARMFIELD W7 model rectangular sedimentation tank. The ultimate goal was to apply efficiency improvements to the geometry of the two tanks through CFD simulations.

The specific aim of this individual study was to provide the group project with a mathematical viscosity model for the CFD simulation. This study was focused on the rheological behaviour of primary sludge which is the by-product of the primary treatment stage of sewage. However, actual primary sludge was not used for the experimental work due to the inherent problems related to handling sewage sludge. Instead, an olive stone powder and water mixture was suggested by Hydro International[®] as a substitute for sewage sludge. From this point onwards that mixture is referred to as the olive stone suspension. The olive stone powder used was purchased from the UK company Goonvean Fibres[®] and was the OSF variety ^{[6][7]}.

The literature review indicated that an olive stone suspension was an acceptable substitute for sewage ^{[3][4][5]}. However, there was a clear gap in existing knowledge regarding the rheology of olive stone suspensions. This was made apparent when a mathematical viscosity model, an important aspect when studying the rheological behaviour of liquids, could not be found for olive stone suspensions in the literature review. This report focused on adding to existing knowledge by providing a mathematical viscosity model that can be used to accurately predict the rheological behaviour of this suspension.

1.1. Waste Water Treatment and Sewage Sludge

Sewage must be treated to prevent chronic ecosystem damage due to oxygen depletion of receiving waters, eutrophication of waters and potential health risks from water-borne pathogens. Sewage also contains litter and solids that must be removed to avoid damage to local wildlife and the environment ^[1]. To diminish these effects, sewage can go through four treatment processes at waste water treatment plants or sewerages: Preliminary, primary, secondary and tertiary treatment ^{[1][2]}.

Preliminary treatment is the removal of grit and gravel by slowing flows down, so matter is deposited in grit traps ^{[1][8][9]}. Primary treatment involves the passive and/or chemically-enhanced process of settlement of suspended solids not removed by preliminary treatment ^{[1][8][9]}. Secondary treatment is the use of bacterial cultures to break down biodegradable matter in waste water ^{[1][8][9]}. Tertiary treatment is used to address several different polluting agents, so it can involve ultra-violet light irradiation (UV treatment), microfiltration or chemical dosing ^[1]. After effective treatment, waste water can be returned to the environment to maintain river flows ^{[1][8][9]}.

During the treatment process an important by-product called sewage sludge is created. There are three main categories: primary, activated and digested sludge ^[2]. Primary sludge, which is the focus of this study, is created during the sedimentation process of primary treatment, contains organic matter and has a large distribution of particle sizes ^[2]. Activated sludge is formed during secondary treatment, contains living and dead bacteria and has a small distribution of particle sizes ^[2]. Finally, digested sludge “has been stabilised by bacteria metabolising the organic material under aerobic or anaerobic conditions” ^[2].

1.2. Properties of Primary Sludge and Olive Stone Powder

Primary and activated sludge has been the focus of several works to understand its rheology ^{[2][10][11][12]}. Primary sludge rheology predicts its behaviour under deformation and can inform the behaviour of sewage treatment plants and primary settling tanks ^{[13][14][15][16]}. In this report the existing knowledge of primary sludge rheology is consolidated and analysed.

However, as mentioned previously, an olive stone suspension was used in this study as a substitute for sewage and primary sludge. Therefore, olive stone suspension rheology was investigated and experimentally analysed through empirical studies. A mathematical viscosity model is provided to predict the rheological behaviour of this suspension.

1.3. Experimental Work

Several experiments were carried out to determine the mathematical viscosity model for the olive stone suspension at the University of Exeter and at Hydro International® facilities. The experimental focus was on determining the following: the *particle size distribution* of the olive stone powder used, the *aspect ratio* of the particles, the *random close-packing fraction* value of the powder and, finally, the rheology of the olive stone suspension. Details of the theory, methodology, error analysis and results of each experiment are presented in sections 3 and 4.

1.4. CFD Simulation

Computational Fluid Dynamics is a tool used to analyse systems which involve fluid flow, heat transfer and associated phenomena by means of computer-based simulation ^[17]. One of the goals of using CFD is to accurately replicate a real-life fluid flow system so that it can be optimised relatively cheaply without having to conduct expensive lab work (i.e. Adjoint Optimisation)^[18]. However, there are two important aspects of CFD simulations to be considered.

Firstly, the difficulty in determining the correct mathematical models to achieve a CFD simulation that can be validated by empirical experiments. The viscosity model of a suspension is one of those models for two-phase flow simulations, the other being the settling velocity of the particles, and requires basic programming knowledge to implement it into the CFD software OpenFOAM®. The main OpenFOAM® solver used in this project was DriftFluxFoam and the viscosity model programming process, specific to this solver, is discussed within the report.

The other aspect is computational cost. If a simulation is highly accurate but takes too long to complete, then the simulation is not a viable tool. The balance between computational time and model accuracy will be investigated by comparing a default suspension viscosity model in DriftFluxFoam known as slurry (which is, in fact, the model proposed by D. Thomas in 1965 ^[19]), to the experimentally determined model for an olive stone suspension described in this report.

1.5. Project Objectives and Deliverables

This study focused on obtaining a mathematical viscosity model that would accurately predict the rheological behaviour of an olive stone suspension and that could be implemented into OpenFOAM[®]. The model was then used in the related group project to create an experimentally validated CFD simulation of a modified rectangular ARMFIELD sedimentation tank and Hydro International's[®] own Swirl-Flo[®] sedimentation tank.

The objectives and deliverables of this report are as follows:

Objectives

- I. Experimentally determine the particle size distribution (PSD) of the olive stone powder purchased from Goonvean Fibres[®].
- II. Experimentally determine the average geometric particle measurements of the olive stone powder particles (i.e. major and minor axis and aspect ratio).
- III. Experimentally determine the random close-packing fraction of the olive stone powder.
- IV. Experimentally determine the rheological behaviour of the olive stone suspension and determine what viscosity model best fits the experimental data.
- V. Introduce the olive stone suspension viscosity model into the computer software OpenFOAM[®] and compare its computational cost to that of the default slurry model.

Deliverables

- I. A mathematical viscosity model that accurately describes the rheological behaviour of an olive stone suspension.
- II. An OpenFOAM[®] viscosity model file for an olive stone suspension.

2. Literature Review

This section looks at previous investigative work related to rheology, suspension viscosity models and the parameters that affect them and the use of CFD as a tool in studies on waste water treatment tanks.

The term rheology was first introduced by Eugene C. Bingham and Markus Reiner to refer to the study of the flow and deformation of all forms of matter ^{[20][21][22]}. A collection of matter (a body) can be described in different states (solids, gases, liquids, etc.). Deformation occurs when a force is applied on a body which alters its shape or size ^{[23][24][25][26]}. Flow occurs when the deformation is continuous for as long as the force is applied or, in other words, when the degree of deformation changes continually with time ^{[23][24][25][26]}.

This deformation and flow is mathematically expressed in viscosity models. These models have three important terms: *shear stress*, *shear rate* and *viscosity* ^{[27][28]}. According to Newton's Law of Viscosity ^{[27][28]} if the shear stress is proportional to the shear rate, then the relationship between the two can be described with the following equation:

$$\tau = \mu \dot{\gamma} \quad (1)$$

Where μ is the property known as *dynamic viscosity* and is expressed in the SI units of Pascal-second (Pa.s). τ is the parameter of shear stress and is expressed in the SI units of Pascals (Pa). $\dot{\gamma}$ is the parameter of shear rate and has the SI units of reciprocal seconds (sec^{-1}).

Any fluid whose flow behaviour can be described with this relationship is called a *Newtonian Fluid* ^{[27][28]}. However, not all fluids are Newtonian, which means they need a different viscosity model to describe their behaviour. These fluids are called *Non-Newtonian fluids* and have been mathematically described by authors such as Bingham ^[29], Ostwald–de Waele ^[30] and Winslow Herschel and Ronald Bulkley ^[31]. The models proposed by these authors differ from Newton's because they have extra parameters that represent different flow and deformation phenomena such as *yield stress* and *flow index*. These models describe different Non-Newtonian fluid behaviour such as that of *Pseudo-Plastic*, *Bingham Plastic*, *Yield Pseudo-Plastic* and *Dilatant* fluids^[27].

In more complex systems the addition of a solid dispersed phase to a Newtonian fluid (a particle suspension) can lead to Non-Newtonian behaviour and require a more complex viscosity model ^[32]. These suspension viscosity models have an additional term called *relative apparent viscosity* ^[32]. This parameter is the ratio of the apparent viscosity of the suspension and the dynamic viscosity of the suspending Newtonian liquid. It is expressed in the following equation:

$$\eta_t = \frac{\eta_s}{\mu_0} \quad (2)$$

Where Eta-t (η_t) is the relative apparent viscosity and is dimensionless. Eta-s (η_s) is the apparent viscosity of the suspension and is expressed in the SI units of Pascal-second (Pa.s). Mu-zero (μ_0) is the dynamic viscosity of the Newtonian suspending liquid and its units are also the Pascal-second.

Relative apparent viscosity is a function of the concentration of solid particles in the system, which is mathematically represented by the *particle volume fraction* and is written with the Greek letter Phi (ϕ).

The addition of particle volume fraction creates a third axis in a standard viscosity curve graph, which traditionally has the x and y axes of shear rate and shear stress, respectively. This extra axis helps describe the change of rheological behaviour of the suspension as more dispersed phase is added to the system (i.e. when the value of ϕ increases).

Early researchers determined that relative apparent viscosity had three distinct regimes of behaviour: dilute, semi-dilute and concentrated ^{[19][33][34]}. The dilute regime is restricted to $\phi \leq 0.01$ for Thomas ^[19] and $\phi \leq 0.02$ for Rutgers ^{[33][34]}. Relative apparent viscosity is approximately linear, and the rheology of the suspension is Newtonian. The semi-dilute regime is restricted to $\phi \leq 0.25$, where η_t shows greater dependence on ϕ but the behaviour of the suspension is still approximately Newtonian ^{[19][33][34]}. Finally, the concentrated regime starts around $\phi = 0.25$ and shows a rapid growth of apparent viscosity and Non-Newtonian behaviour as particle volume fraction increases ^{[19][33][34]}.

The first person to describe the rheological behaviour of suspensions in the dilute regime was Einstein in 1911 ^[35]. He analytically derived the solution of the hydrodynamic flow around a sphere:

$$\eta_t = 1 + B\phi \quad (3)$$

Where B is the *Einstein coefficient* and was given a value of 2.5 by Einstein ^[35]. Other researchers have placed this coefficient between the range of 1.5 and 5, meaning that the model has not been completely validated ^{[36][37][38][39]}.

In addition to this uncertainty, Einstein's model is highly impractical because it is only applicable within the dilute suspension regime ^{[19][33][34]}. To overcome this, work has been done in the semi-dilute regime to determine coefficients of the higher order terms in ϕ . This work has produced equations that follow the following structure:

$$\eta_t = 1 + B\phi + B_1\phi^2 + \dots \quad (4)$$

Where B has a value of 2.5 and B_1 can take different values depending on the considerations of particle-particle interactions ^{[40][41][42]} and *Brownian motion* ^{[43][44]}. These polynomial relationships are applicable within the dilute and semi-dilute regime but are inaccurate within the concentrated regime ^[32]. Mueller et al. say that one reason for this is that the polynomial relationships predict a finite value of viscosity as ϕ approaches a value of one. However, as stated by S. Mueller, this does not make physical sense as the densest possible packing of any type of particle is never one ^[32]. For example, for spherical monodisperse particles the highest particle volume fraction (i.e densest possible packing) achievable is approximately $\phi = 0.74$ ^[32]. This means that once the particle concentration reaches this value, viscosity must be infinite ^[32]. This point of divergence of the relative apparent viscosity is commonly referred to as the *maximum packing fraction*.

Maximum packing fraction is defined as the densest possible configuration of particles inside a volume of reference. The value is dependent on particle shape, size distribution and type of packing ^{[32][45][46][47]}. This means that the most accurate suspension viscosity models for the concentrated regime have the maximum packing fraction of the dispersed phase as a parameter ^[32]. The most commonly used equation that has the maximum packing fraction as a parameter is the Krieger & Dougherty relationship, where the value is changed to fit experimental data ^[48].

$$\eta_t = \left(1 - \frac{\phi}{\phi_m}\right)^{-B\phi_m} \quad (5)$$

Where ϕ_m and B are fitting parameters to experimental data in regression analysis (i.e. there values are changed to fit experimental data) ^{[38][39]}. Other equations have been proposed by authors such as: Roscoe^[49], Maron and Pierce^[50], Thomas^[19], Chong et al.^[51], Batchelor^[44], Dabak and Yucel ^[52], Liu^[53], Costa^[54], Boyer et al^[55] and as recently as 2017 Zhu et al.^[56].

These models are used to predict the behaviour of suspensions, however regression analysis to experimental data is required to determine their accuracy to specific suspensions.

The instruments used to experimentally measure flow properties of fluids are named rheometers and viscometers ^{[23][24][25][26]}. These measuring instruments range from rotational rheometers, capillary viscometers, falling and rolling ball viscometers, rising bubble viscometers, among others, each with their own physical theory and equations ^{[23][24][25][26][28]}. However, all of these instruments face a common issue with the measuring of suspension rheology, which is the rapid settling of particles in unstable mixtures ^{[24][58]}. Solutions for measuring unstable suspensions range from suspension agitation ^[58], special stirring mechanisms^{[59][60][61]} and more viscous Newtonian suspending mediums ^{[32][62]}.

Once the viscosity model is known, it is programmed into the CFD software of choice. Authors who have done this for wastewater treatment tanks are: Dahl^[13], Liu and Garcia^[16] and Brennan^[15]. The viscosity models they used were based on studies performed by R. Dick and B. Ewing^[10] and T. Papanastasiou^[57]. Another viscosity model for primary, activated and tertiary sludge has also been proposed by S. N. Little^[2]. These models proposed that the behaviour of sludge was dependent on particle volume fraction and are Non-Newtonian.

Authors have described the need for Non-Newtonian viscosity models for sludge^{[63][64]}, however, there is no agreement on the specifics of the model, except that it must be Non-Newtonian. This disagreement is probably due to the fact, as detailed by S. N. Little, that the sludges studied by each researcher do not all have the same properties ^[2]. This indicates that the viscosity model chosen for the olive stone suspension must be dependent on the particle volume fraction and ideally be Non-Newtonian.

Past work of suspension rheology showed a clear path for the project work. The olive stone particles needed to be analysed to determine their particle size distribution, shape and random close-packing fraction. This data would categorise how the particles behave in water and help validate the viscosity model chosen from a rheological study. The viscosity model would then be provided to the wider-ranging group project members so that it could be introduced into the CFD software OpenFOAM[®] which would produce simulation results of two sedimentation tanks, Swirl-Flo[®] and a modified ARMFIELD rectangular tank ^{[65][66]}. The simulations would then be compared with empirical results obtained in the Exeter University Fluids Lab to validate the choice of viscosity model for the olive stone suspension ^[67].

3. Theoretical Background and Experimental Work

This section elaborates on the key theoretical areas regarding rheological analysis of a powder/water suspension, giving an outline of the governing equations and the parameters of rheology and suspension viscosity. Then follows the outline, theory and methodology of all the experimental work carried out in the project. Finally, the methods used to determine what viscosity model was the most appropriate for the olive stone suspension and the resulting OpenFOAM® programming methodology are discussed.

3.1. Governing Equations

3.1.1. Newtonian and Non-Newtonian Fluids

Viscosity is defined as the measure of a fluid's resistance to flow and can be generally defined by the shearing of a fluid between two parallel plates as seen in Figure 1.

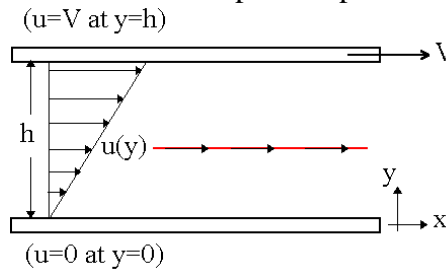


Figure 1: Fluid Between Two Parallel Plates ^[68]

A velocity gradient develops across the space between the two plates because the top plate is moving, and the bottom plate is stationary ^{[27][28]}. The velocity gradient is the measure of velocity at which the fluid layers move with respect to each other ^{[27][28]}. It is the description of the shearing effect that is being experienced by the fluid ^{[27][28]}. It is called shear rate; its unit of measure is the reciprocal second (s^{-1}) and it is represented by the following equation.

$$\dot{\gamma} = \frac{(x/t)}{y} = \frac{u}{y} = \frac{du}{dy} \quad (6)$$

The force per unit area (F/A) that is required to create the shearing of the fluid is called shear stress^{[27][28]}. Its unit of measure is the Newton per square meter (N/m^2) or as it more commonly known, the Pascal (Pa) and it is represented by the following equation.

$$\tau = \frac{F}{A} \quad (7)$$

If the assumption is made that the shear stress is proportional to the shear rate, then the following expression can be written.

$$\tau = \mu \dot{\gamma} \quad (1)$$

This is known as Newton's law of viscosity^{[27][28]}. Fluids that obey this law of viscosity are known as Newtonian fluids^{[27][28]}. Common fluids such as water and air are examples of Newtonian fluids and each has its own value of dynamic viscosity^{[27][28]}. However, fluids that do not obey Newton's law of viscosity are called Non-Newtonian fluids and their viscosity is a function of shear rate or shear rate history^[27]. These special fluids can be classified as time-independent or time-dependant based on whether their viscosity is a function of shear rate or *shear rate history*, respectively^[27].

Time-independent, Non-Newtonian fluids do not vary their rheological properties with time and their viscosity is a function of shear rate^[27]. Different types of time-independent, Non-Newtonian fluids are dilatant, pseudo-plastic, Bingham Plastic and yield pseudo-plastic^[27].

On the other hand, a time-dependent, Non-Newtonian fluid is dependent on the shear rate history of the fluid (i.e. how long shear has been applied) and can be classified as Thixotropic or Rheopectic. A Thixotropic fluid's dynamic viscosity decreases after a constant shear rate has been applied for a certain amount of time, while for a Rheopectic fluid the dynamic viscosity increases^[27].

Time-independent, Non-Newtonian fluid behaviour is described with mathematical models called viscosity models. The most common models are the Herschel-Bulkley^[31] and Power Law models^[30]. For the Herschel-Bulkley model, the shear stress must reach a minimum value before flow starts (i.e shear stress of 5Pa in Figure 2). This value is called the *yield stress* and the model is described with the following equation.

$$\tau = \tau_0 + K \dot{\gamma}^n \quad (8)$$

The terms tau zero (τ_0), K and n are yield stress, consistency and flow index, respectively. Where the yield stress has the units of Pascal (Pa), consistency has the units of Pascal-second (Pa.s) and flow index is dimensionless.

If n is equal to one (1) then the fluid is a Bingham Plastic and the viscosity value after yield stress is called the *plastic viscosity*^[27]. However, if n is lower than one (1) then the fluid is called a Yield Pseudo-Plastic and is *shear-thinning* because viscosity decreases as shear rate increases^[27].

For the Power Law model there is no value for yield stress. The shear stress vs. shear rate relation is described by the following equation.

$$\tau = K \dot{\gamma}^n \quad (9)$$

If the value of n is equal to one (1) then the fluid is Newtonian^[27]. If the value of n is lower than one (1) then the fluid is a Pseudo-plastic and shear thinning^[27]. However, if n is higher than one (1) then the fluid is a Dilatant substance and *shear-thickening*, where the dynamic viscosity increases as the shear rate increases^[27].

The difference between Newtonian and time-independent Non-Newtonian fluids can be visualized in Figure 2 below. This is a viscosity curve graph where the x-axis is the shear rate and the y-axis is the shear stress.

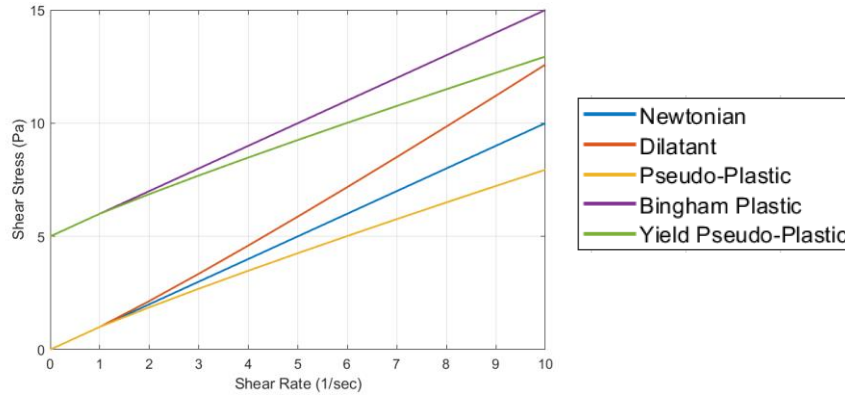


Figure 2: Viscosity Curve Graph of Newtonian and Time-independent Non-Newtonian Fluids

In more complex systems the addition of a dispersed phase to a Newtonian fluid (a suspension) can lead to Non-Newtonian behaviour and require a more complex viscosity model than the ones mentioned previously^[32].

3.1.2. Suspension Rheology and Factors That Affect It

Complex fluid systems such as emulsions (liquid-liquid), bubble suspensions (gas-liquid) or solid particle suspensions (solid-liquid) have different factors that affect their rheology. Specifically, for particle suspensions, these factors are the concentration of particles in the fluid, the properties of the particles such as shape, size distribution, type of packing and finally interparticle interaction and attraction (i.e. electroviscous effects)^[32]. The most important factor that affects suspension rheology is the concentration of solid particles in the system. This concentration is mathematically determined by the particle volume fraction:

$$\phi = \frac{V_p}{V_f + V_p} = \frac{(M_p/\rho_p)}{(M_f/\rho_f) + (M_p/\rho_p)} = \frac{\text{Concentration } (\frac{mg}{l})}{1000 \times \rho_p} \quad (10)$$

Where V , M and ρ are the volume, mass and density respectively, and their units are cubic metres (m^3) for volume, Kilogram (Kg) for mass and Kilogram per cubic metre (Kg/m^3) for density. The subscript p indicates the value related to the dispersed phase (particles) and f indicates the value related to the fluid phase (water) of the suspension.

The effect of particle volume fraction on the viscosity of the suspension is mathematically expressed by the concept of relative apparent viscosity^[32]. This parameter is the ratio of the apparent viscosity of the suspension and the dynamic viscosity of the suspending Newtonian liquid and is described in the following equation.

$$\eta_t = \frac{\eta_s}{\mu_0} \quad (2)$$

Where η_s is the apparent viscosity of the suspension, μ_0 is the dynamic viscosity of the Newtonian suspending medium and η_t is a function of particle volume fraction ϕ . The relative apparent viscosity equation can be re-written to determine the shear stress and shear rate relationship of suspensions

$$\tau = \eta_s \dot{\gamma} = \mu_0 \eta_t \dot{\gamma} \quad (11)$$

This equation describes Newtonian suspension rheology. More complex models include a parameter for yield stress and flow index which are functions of particle volume fraction^[32].

Another important factor to be considered is that suspension viscosity models have distinct regimes of behaviour: Dilute, Semi-Dilute and Concentrated^{[19][33][34]}. Different suspension models have been proposed and have had varying success when it comes to predicting the behaviour of suspensions in the different concentration regimes^[32]. The most accurate models have been those that have the parameter of maximum packing fraction^[32]. The mathematical description of this parameter is as follows:

$$\phi_m = \frac{V_{\text{maximum volume of particles}}}{V_{\text{reference volume}}} \quad (12)$$

This value is dependent on the particle shape, size distribution and type of packing^[32], showing that it is important to understand the particle shape and size distribution of the particles in the solid particle suspension that is being studied.

The shape of a particle can be determined from its aspect ratio^[69]. The aspect ratio is the ratio between the major and minor axis of the best fitting ellipse to the particle shape^[69]. Where for a perfectly spherical particle the value of the aspect ratio is equal to one (1), for an oblate particle the aspect ratio is less than one (1) and for a prolate particle the aspect ratio is greater than one (1)^[69].

It is documented that particles of an aspect ratio of one (i.e. spheres) have a higher packing fraction than prolate particles^[32], (i.e. they pack more densely).

$$r_p = \frac{\text{Major Axis}}{\text{Minor Axis}} = \frac{l_a}{l_b} \quad (13)$$

It is also documented that the value of the densest possible packing fraction for monodisperse spheres is approximately $\phi_m = 0.74$ ^[32]. However, if the particles are packed randomly (i.e. random-close packing), as is normal for suspensions, the value gets closer to approximately $\phi_m = 0.64$ ^[32]. This means that if the particles in the suspension are prolate, the value of ϕ_m should be lower than 0.64, because the particles would be packed randomly. This *random close-packing fraction* can be predicted by fitting viscosity models to rheological experimental data or by randomly pouring the particles into a container of known volume.

The aspect ratio of the particles also has additional effects on the viscosity of the suspension. The flow around a non-spherical particle is different to that around a spherical one, so the contribution of the individual particle to viscosity will also be different^[32]. Moreover, non-spherical particles are orientable, so their contribution to suspension viscosity is dependent on their orientation^[32]. Finally, the interaction between particles (i.e. electroviscous effects) is greater for non-spherical particles than spherical ones^[32].

The size distribution of the particles is important because *polydisperse systems* (i.e. several particle sizes^[70]) have higher packing fraction values than *monodisperse systems* (i.e. one particle size^[70]) because smaller particles can be packed more efficiently by layering themselves against larger particles or by falling into the spaces created by larger neighbouring particles ^[47].

The size of the particles also determines other key factors in the suspension: firstly, their subdivision name (i.e. *colloid* for particles between 1 nanometre (nm) and 1 micrometre (μm) in size, and *granule* for particles between $50\mu\text{m}$ and $200\mu\text{m}$ ^[70]); secondly, the impact of Brownian motion (i.e. random movement of particles that most notably affects colloidal suspensions^[70]) which is determined by the dimensionless Peclet number^{[71][72][73]} and finally, the coupling between the solid and fluid phases which is determined by the dimensionless Stokes number^[74]. The two dimensionless numbers mentioned above can be written in the following equations:

Table 1: Dimensionless Numbers Dependent on Particle Size

Peclet Number ^[32] (Eq. N: 14)	Stokes Number ^[32] (Eq. N: 15)
$Pe = \frac{6\pi\mu_0 a^3 \dot{\gamma}}{kT}$	$St = \frac{\rho_p a^3 \dot{\gamma}}{\lambda\mu_0}$

Where a is the particle radius in metres (m), k is the Boltzmann constant which is equal to 1.38×10^{-23} Joules per Kelvin (J K^{-1}), T is the temperature of the suspending liquid in Kelvin

(K) and Lambda (λ) is the characteristic length of the particles in metres (m)^[32]. These numbers are important because at $Pe \geq 10^3$ Brownian motion is interrupted by hydrodynamic forces^{[73][72][75]} and variations in the Stokes number may lead to non-Newtonian behaviour^[74]. Additionally, at low Stokes numbers (i.e. $St \ll 1$) the coupling between the particle and fluid phase of the suspension is strong^[32], meaning that the particles follow the flow of the fluid they are suspended in.

3.1.3. Suspension Viscosity Models

Several equations have been proposed for relative apparent viscosity by different authors, a small collection of the most relevant ones to this project can be seen in Table 2.

Table 2: Proposed Equations for Relative Apparent Viscosity

Author (Year)	Equation	Applicable Region	Eq. N
Einstein (1911) ^[35]	$\eta_t = 1 + 2.5\phi$	Dilute	(3)
Roscoe (1952) ^[49]	$\eta_t = \left(1 - \frac{\phi}{\phi_m}\right)^{-2.5}$	Dilute to Concentrated	(16)
Maron & Pierce (1956) ^[50]	$\eta_t = \left(1 - \frac{\phi}{\phi_m}\right)^{-2}$	Dilute to Concentrated	(17)
Krieger & Dougherty (1959) ^[48]	$\eta_t = \left(1 - \frac{\phi}{\phi_m}\right)^{-B\phi_m}$	Dilute to Concentrated	(18)
Thomas (1965) ^[19]	$\eta_t = 1 + 2.5\phi + 10.05\phi^2 + 0.00273e^{(16.6\phi)}$	Dilute to Semi-Dilute	(19)
Chong (1971) ^[51]	$\eta_t = \left(1 + 0.75 \frac{\phi/\phi_m}{1 - (\phi/\phi_m)}\right)^2$	Dilute to Concentrated	(20)
Batchelor (1977) ^[44]	$\eta_t = 1 + 2.5\phi + 6.2\phi^2$	Dilute to Semi-Dilute	(21)
Dabak (1986) ^[52]	$\eta_t = \left(1 + \frac{2.5\phi\phi_m}{2(\phi_m - \phi)}\right)^2$	Dilute to Concentrated	(22)

In Table 2 the terms ϕ_m and are called fitting parameters as they are changed to match rheological experimental data. By doing this, the viscosity models can predict what the maximum packing fraction of the studied particles is. Unfortunately, these equations only describe Newtonian suspensions as seen in equation 11, which means they lack a term for yield stress or flow index, which are important for concentrated suspensions^[32]. This issue was addressed by Thomas by describing the following modified Bingham Plastic model, where the yield stress and plastic viscosity are functions of particle volume fraction^[76]:

$$\tau_y = k_1\phi^3 \quad (23)$$

$$\eta = \mu_0 e^{k_2\phi} \quad (24)$$

Where k_1 and k_2 are fitting parameters, ϕ is the particle volume fraction and μ_0 is the dynamic viscosity of the suspending medium. Unfortunately, these equations can only be applied up to the semi dilute region of suspensions. Mueller also described the following modified Herschel-Bulkley model, where the yield stress, consistency and flow index are functions of the particle volume fraction^[32]:

$$\tau_y = \tau^* \left(\left(1 - \frac{\phi}{\phi_m} \right)^{-2} - 1 \right) \quad (25) \quad K = \mu_0 \left(1 - \frac{\phi}{\phi_m} \right)^{-2} \quad (26)$$

$$n = 1 - 0.2r_p \left(\frac{\phi}{\phi_m} \right)^4 \quad (27) \quad \phi_m = \frac{2}{0.321r_p + 3.02} \quad (28)$$

Where τ^* is a fitting parameter, ϕ is the particle volume fraction, μ_0 is the dynamic viscosity of the suspending medium and ϕ_m is a function of r_p which is the average aspect ratio of the particles. This suspension viscosity model can be used in the dilute, semi-dilute and concentrated regime^[32]. In this study, these viscosity models were compared to experimental data to determine the most accurate in describing the rheology of the olive stone suspension. Other experimental work was done on the olive stone particles by determining their size distribution, aspect ratio and random close-packing fraction to validate the model chosen.

3.2. Experimental Work

3.2.1. Particle Size Distribution of Olive Stone Powder

Outline

The objective of the experiment was to determine the particle size distribution (PSD) of olive stone powder and prepare samples for microscope analysis. This was achieved by using a mechanical shaking sieve with different sized sieves stacked on top of one another.

Theory

Particle size distribution is the list of values or mathematical function that defines the number of particles present in a sample according to their size. Knowing the PSD of a sample allows important characteristics to be determined, i.e. the degree of polydispersity and mean particle size. The best way to determine the PSD of a sample is by using a Sedigraph, which uses the concept of Stokes' Law and Beer-Lambert-Bouguer Law^[77]. Consequently, the Sedigraph at the University of Exeter's Geography department was initially chosen to determine the PSD.

However, during the routine pre-treatment it was observed that the particles were destroyed

and substantially altered, leaving only a trace white sediment. The procedure involved adding a small amount of concentrated Hydrogen Peroxide (H₂O₂), followed by heating the suspension to approximately of 90°C to increase the speed and completeness of peroxide oxidation of the sample. H₂O₂ was added to destroy all organic matter in the sample, a step required for the determination of particle size distribution of soils and sediments because organic matter is known to bind particles together. Since olive stone particles are organic, it was deemed by the technicians involved that the Sedigraph was not suitable for this experiment.

Hence, a sieving method was chosen instead to determine the PSD. In accordance with BS EN 933-1:2012^[78], the sieving test consists of dividing and separating a material into several particle size classifications of decreasing sizes by means of a series of sieves. The material retained in each sieve is weighed and recorded. The percentage of the material retained in each sieve and the pan is calculated with the following equation.

$$\text{Material Retained (\%)} = \frac{100xR_i}{M_1} = \frac{100xP}{M_1} \quad (29)$$

Where R_i and P is the amount of material retained on a sieve size or the pan and M_1 is the total dry mass of the sample that is being analysed. All these measurements are done in grams (gr). The cumulative percentage of the original dry mass sample passing each sieve can be calculated with the following equation.

$$\text{Cumulative Percentage Passing (\%)} = 100 - \sum \frac{100xR_i}{M_1} \quad (30)$$

$$\text{Cumulative Percentage Retained (\%)} = \sum \frac{100xR_i}{M_1} \quad (31)$$

The results from the sieve test can be validated with the following equation.

$$\text{Validation Percentage (\%)} = \frac{M_1 - (\sum R_i + P)}{M_1} \times 100 \quad (32)$$

If the validation percentage is above 1%, the test must be repeated.

Methodology

0.2 Kilograms of olive stone powder was weighed on a sartorius™ digital scale and recorded as M_1 . Five different sieves were placed in descending order of aperture size on a Retsch™ mechanical sieve shaker with aperture sizes of 250µm, 125µm, 63µm, 45µm and 32µm with a pan underneath the last sieve. The top of the sieve shaker was secured, and the machine was set to run for ten minutes at an amplitude of 1mm. After ten minutes the powder within the

five sieves and pan were removed and weighed individually. The experiment was repeated three times to account for errors in procedure.

3.2.2. Average Particle Geometry of Olive Stone Powder

Outline

The objective was to determine the average shape of the olive stone particles, particularly their aspect ratio. This was done by taking pictures of the particles with a Scanning Electron Microscope (SEM) and then manually measuring the particles.

Theory

Particle size characterisation with microscopy-based techniques offers a powerful tool for the determination of particle size, size distribution and morphology^[69]. Particle shape and size is determined by measuring the particle directly and calculating the size based on a defined measure of diameter^[69]. The calculated sizes are expressed as the measurements of an ellipse that has the same projected area as the projected image of the particle^[69].

The instruments used for microscopy-based techniques include optical light microscopes, scanning electron microscopes (SEM) and transmission electron microscopes (TEM). Factors determining the choice of instrument to be used are size range of the powders being studied, magnification, and resolution that is desired^[69]. In accordance with BS 3406-4:1993^[79], optical light microscopes are suitable for the measurement of particles in the size range of 3 μm to 1mm, SEM for 20nm to 1mm and TEM for 2nm to 1 μm ^[79]. Given that the size distribution of olive stone powder reported on the Goonvean Fibres[®] data sheet was a minimum particle size of 75 μm ^[6], an SEM microscope was chosen for particle analysis.

An attempt was made to use an opensource image analysis software (ImageJ). Although this type of software was not readily available at the University of Exeter Imaging Suite, its use was suggested by a technician. However, the ImageJ did not work with the resolution of the images obtained at the lab. This forced the manual measuring of the particles.

Methodology

A pre-classified size distribution sample from sieving was placed on small pieces of carbon tape and the excess powder was removed with pressurized air. The samples were coated in a five-nanometre layer of a platinum and palladium mixture. All the samples were placed within the SEM microscope sample chamber in different positions. The microscope was

pressurized and prepared. Each sample region was located on a computer display and then magnified until it was in focus. Several pictures were taken, printed and then measured by hand.

3.2.3. Random Close-Packing Fraction of Olive Stone Powder

Outline

The objective of the experiment was to empirically determine the random close-packing fraction of olive stone powder, which would then be used to compare with the predicted value from the viscosity models. This was accomplished by filling two empty containers (box and sphere) of known volume with olive stone powder while being shaken. Ball bearings were used to validate the experimental procedure, as the random close-packing fraction for these types of particles is known to be approximately 0.64^[32].

Theory

Random close-packing fraction is the empirical parameter that is used to characterise the maximum volume fraction of solid objects packed randomly. It is calculated via an experiment involving the shaking of a container of powder. As the container is shaken, the volume of powder inside the container is reduced, allowing for more powder to be added to the container. However, a limit is reached, and additional powder cannot be added which means that the densest arrangement of particles packed randomly has been obtained. At this point the mass of the powder in the container is calculated M_p in Kilograms (Kg). so that the random close-packing fraction can be calculated with the following expression.

$$\phi_{rcp} = \frac{V_{particles \text{ in the container}}}{V_{empty \text{ container}}} = \frac{M_p / \rho_p}{V_{empty \text{ container}}} \quad (33)$$

Where the M_p is the mass of randomly packed particles in a container and ρ_p is the density of the particles. The density of the olive stone powder used was calculated as 1438.1 ± 102.9 Kg/m³ by another member of the group project^[80]. Therefore, this experiment was concerned with calculating M_p in Kilograms (Kg) with the following equation:

$$M_p = M_{full} - M_{empty} \quad (34)$$

Where M_{empty} in Kilograms (Kg) is the mass of the empty container and M_{full} in Kilograms (Kg) is the mass of the full container.

Methodology

The maximum volume inside a box and sphere container was recorded as V_{empty} in cubic metres (m^3). Each was weighed individually on a Kern PCB digital scale and its mass recorded as M_{empty} in Kilograms (Kg). The olive stone powder was poured into the containers until they were filled to a known volume. The container was shaken during the filling procedure to ensure maximum packing was achieved. The full box and sphere were then weighed again on the same digital scale and the mass recorded as M_{full} in Kilograms (Kg). M_p in Kilograms (Kg) could then be calculated. The weight was then converted into volume by dividing it by the calculated density of olive stone powder. The maximum packing fraction was determined by dividing the volume occupied by the olive stone powder by the volume of the container. The above steps were repeated three times and then again for monodisperse spherical ball bearings.

3.2.4. Rheology of an Olive Stone Suspension

Outline

The objective of the experiment was to determine the rheological behaviour of an olive stone suspension at different powder concentrations. This was accomplished by using a Brookfield digital coaxial rotating rheometer with a Vane spindle. The viscosity models from Table 2 and equations 23 to 28 were then fitted to the experimental data to determine which one was the most accurate in describing the rheological behaviour of the olive stone suspension.

Theory

The basic theory of rotational rheometers is that a rotating body, or spindle, is immersed in a liquid and experiences a viscous drag or retarding force. The amount of viscous drag is a function of the speed of rotation of the body. This is recorded by the rheometer as shear stress and shear rate which are terms used to calculate the viscosity of the fluid^{[24][28]}.

In the case of the LVDV-III Ultra used for this project, the principle of operation is to drive a spindle through a calibrated spring^[81]. The viscous drag of the fluid against the spindle is measured by the spring deflection^[81]. Spring deflection is measured with a rotary transducer^[81]. The viscosity measurement is determined by the rotational speed of the spindle, the size and shape of the spindle, the container the spindle is rotating in, and the full-scale torque of the calibrated spring^[81].

The LVDV-III Ultra has several experimental methodologies to determine rheological

behaviour. These include the following, all of which were used for this study: Firstly, Up-Down Rate Ramp, a test that consists of increasing shear rate in set value intervals until a maximum is reached and then reducing the shear rate in the same intervals. This is to determine the shear stress and shear rate relationship of the liquid^[82]. Secondly, Time Sensitivity Test, where a fixed shear rate is chosen and applied for a set amount of time. This is to determine the time dependence of the liquid^[82]. Thirdly, the EZ-Yield Method, where a low shear rate is chosen and applied for a set amount of time. The maximum torque value is recorded and the yield stress is calculated^[82].

Methodology

A 600ml beaker (5cm radius) was filled with 500 ml of tap water (20°C). Vane spindle 72 (1.084cm radius and 4.333cm effective length) was connected to the rheometer. The guard leg of the rheometer was left on. An Up-Down Rate Ramp test was done by setting the rheometer to increase its RPM in intervals of 2.07 for 90 seconds until a maximum of 60 RPM was reached, then for another 90 seconds the RPM was lowered in intervals of 2.07. A time sensitivity test was done by setting the rheometer RPM to a fixed value (2 RPM) for 56 seconds. A yield stress test was done by setting the rheometer to an RPM of 0.3 for 1 minute. The highest attained torque measurement (%) was recorded. The above steps were done for the following particle concentrations: 0g/l, 5g/l, 10g/l, 15g/l, 20g/l, 30g/l, 150g/l, 300g/l and 450g/l. Different suspension viscosity models were fit to the experimental data using regression analysis to determine which one described the behaviour most accurately.

3.3. CFD Simulations and OpenFOAM® Programming

The CFD software used in the group project to simulate a sedimentation tank with an olive stone suspension was the opensource CFD software OpenFOAM®. It is a Linux based C++ library, which is used to create executables know as applications^[83]. The applications fall into two categories: *solvers*, which are used to solve a specific problem in continuum mechanics and *utilities* which perform tasks involving data manipulation^[83]. New solvers and utilities can be created with pre-requisite knowledge of underlying method, physics and programming techniques, which are then used in the general OpenFOAM® structure seen in Figure 3.

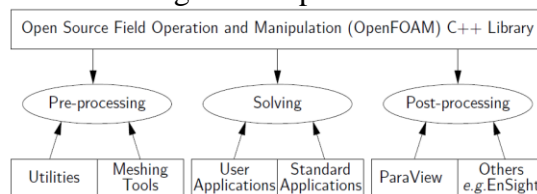


Figure 3: OpenFOAM® Structure ^[83]

In the pre-processing stage the geometries, meshes, case files and user created applications are prepared. In the solving stage specific applications are chosen to solve the specific continuum mechanics problem. In the post-processing stage relevant information is extracted from the simulation which is then compared to empirical results from experiments, which is used to validate the simulation.

In the overarching group project, work was done in each step of the OpenFOAM[®] structure to reach a validated simulation. This work included mesh quality and case file inputs in the pre-processing stage^{[80][85][86]}, solver characteristic analysis ^{[65][66]} in the solving stage and finally simulation validation in the post-processing stage^[67]. The work done in this report is focused on the modification of an existing solver to include a new suspension viscosity model, which fits in the pre-processing and solving stage.

The solver used in the group project was `DriftFluxFoam`, which is designed for two (2) incompressible fluids using the mixture approach with the drift-flux approximation for relative motion of the phases^[83]. For this study, the two incompressible fluids were the suspending Newtonian medium (water) and the olive stone suspension.

The `DriftFluxFoam` solver requires a viscosity model for both the suspending medium and the suspension. These two models are picked by the user in the `transportProperties` file of a normal OpenFOAM[®] case file. The suspending medium model is normally set to Newtonian and the suspension model is normally dependent on the value of particle volume fraction.

The OpenFOAM[®] version 2.4.0. solver used for this report comes with four standard viscosity models for the suspension: Bingham Plastic, `mixtureViscosityModel`, plastic and slurry. All four are functions of the particle volume fraction and, notably, the slurry model was found to be the Thomas model described in equation 19.

Based on this fact, together with the considerations that the slurry model did not require any experimentally determined constants and that it was already installed in the software, it was decided that it would be a good starting point for the initial CFD simulations while the viscosity model specific to the olive stone suspension was being determined. However, to use the model the assumption had to be made that the particles are spherical, the suspension is Newtonian and that the particle volume fraction in the simulation does not reach a value higher than that of the semi-dilute regime.

Ultimately, a comparison of this existing slurry model would be done with the viscosity model specific to the olive stone suspension obtained in this study, once the latter had been introduced into the OpenFOAM® software. The model comparison would be done at a point where both the simulations and empirical experiments had reached a *steady state*. This is the point in time where parameters within the continuum mechanics problem stop changing with time (i.e. the mass flow rate leaving the tanks, the velocity profiles, the amount of dispersed phase within the tank, etc.).

However, for this to be possible all other aspects of the OpenFoam® structure had to remain constant (i.e. mesh geometry, case file inputs, simulated time, etc) while only changing the viscosity model. But, due to the iterative nature of the group project, time consuming setbacks and lack of computational power, this point of comparison could not be reached. Consequently, it was decided that the computational cost of the models would be analysed and compared. The computational cost comparison would be made according to how long it took for each model to reach steady state in the CFD simulation.

3.3.1. Introducing a New Viscosity Model

Once the appropriate viscosity model was chosen for the olive stone suspension, it had to be programmed into the software OpenFOAM®. The solver used was `DriftFluxFoam` and its file structure is described in the following methodology. The viscosity model programming methodology in OpenFOAM® has the steps seen in Figure 4.

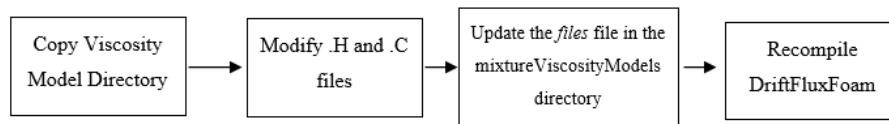


Figure 4: Viscosity Model Programming Methodology in OpenFOAM®

The process of introducing a new model is as follows. For the sake of explanation, the relevant file structure of the `DriftFluxFoam` directory is presented in Figure 5.

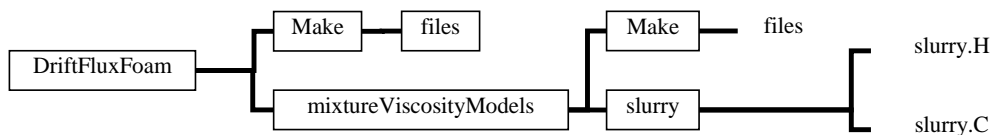


Figure 5: DriftFluxFoam Solver Directory Structure

Inside the `DriftFluxFoam` directory there is a sub-directory called `mixtureViscosityModels` with four viscosity model folders called: Bingham Plastic,

mixtureViscosityModel, plastic and slurry. Another sub-folder within the mixtureViscosityModels folder is the Make folder. For the sake of explanation, the new viscosity model name is Newvisc.

The first step was to copy the slurry folder and paste it in the same mixtureViscosityModels directory and then rename it to the relevant model name, which for the sake of explanation, is Newvisc.

Within the new viscosity model folder there were two files called `slurry.H` and `slurry.C`. Firstly, the files were renamed to `Newvisc.H` and `Newvisc.C` and any instance of `slurry` within the files themselves was changed to `Newvisc`. The next step was to change the details of the `.H` and `.C` files.

In the `.H` file any constants and parameters in the model needed to be declared. In the `.C` file the dimensions of the constants are specified, and labels are created for them. The labels are the words that the OpenFOAM® software looks for in the `transportProperties` file when running a simulation. Within the `.C` file the member function is altered to reflect the structure of the viscosity model. Once the `.H` and `.C` files have the proper adjustments the `files` file in the `Make` directory inside the `mixtureViscosityModels` directory is updated to include the new viscosity model. Once all the documents are up to date, the `DriftFluxFoam` solver can be recompiled. This is done by typing `./Allwclean` in a terminal window while in the `DriftFluxFoam` directory to clear any dependencies and then typing `./Allwmake` to recompile the solver. Once this has been done the newly created viscosity model is added to the `DriftFluxFoam` solver.

3.4. Results Analysis

This section explains how the data obtained in this study was analysed so that conclusions from each experiment and simulation could be reached.

The particle size distribution from the sieve shaker experiment would determine a particle size range of interest (i.e. the range where the largest amount of powder was located). Firstly, this range would permit the classification of the particles (i.e. the particles would be determined to be colloidal or granule). Secondly, it would determine the behaviour of the particles in water (i.e. the Peclet and Stokes number) which determines if the suspension would be susceptible to Brownian motion and the theoretical degree of coupling between the particle and fluid phase of the suspension.

The average aspect ratio of the particles from the previously determined range of interest, would be determined with the SEM microscope. This would then be used in the Mueller viscosity model, equation 27 and 28, and would further classify the behaviour of the particle suspension (i.e. inter particle interactions and the approximate value of the maximum packing fraction).

The random close-packing experiments would serve as an empirical point of comparison for the predicted value of maximum packing fraction predicted by the viscosity models in Table 2 and equations 23 to 28.

The rheological experiments would classify the behaviour of the olive stone suspension. Regression analysis would be used to fit the viscosity models from Table 2 and equations 23 to 28 to the data obtained from the Up-Down rate ramp. The time sensitivity test would determine if the suspension was dependent on shear rate history and time. The yield test would determine the value of yield stress for the suspension at different concentrations.

The CFD simulations in the OpenFOAM[®] software of both the Swirl-Flo[®] and modified ARMFIELD rectangular sedimentation tanks, would determine the computational cost of both the chosen viscosity model and the standard slurry model, equation 19, to reach the steady state time measured in the empirical experiments performed on the same tanks in the University of Exeter Fluids Lab.

4. Presentation of Experimental and CFD Results

4.1. Particle Size Distribution of Olive Stone Powder

Table 3: Results From Sieve Shaker Experiment

Sieve Aperture Size (µm)	Material Retained (gr) ± 0.005gr			Percentage Retained			Cumulative Percentage Passing			Cumulative Percentage Retained		
	Test 1	Test 2	Test 3	Test 1	Test 2	Test 3	Test 1	Test 2	Test 3	Test 1	Test 2	Test 3
250	1.09	0.94	1.04	< 1%	< 1%	< 1%	99%	100%	99%	< 1%	< 1%	< 1%
125	2.42	3.18	1.92	1%	2%	1%	98%	98%	99%	2%	2%	1%
63	61.56	59.40	58.26	31%	30%	29%	67%	68%	70%	33%	32%	30%
45	72.94	72.61	72.83	36%	36%	36%	31%	32%	33%	69%	68%	67%
32	52.57	55.18	57.88	26%	28%	29%	5%	4%	5%	95%	96%	95%
Pan	7.86	7.44	7.23	4%	4%	4%	<1%	< 1%	< 1%	99%	99%	99%
Total initial dry mass (Test 1, Test 2 and Test 3), M ₁ = 200.05gr, 200.00gr, 201.00gr ± 0.005gr												
Percentage Loss = 0.8%, 0.6%, 0.9% < 1%												

Data and Error Analysis

Table 3 shows the in all three experiments most of the powder was retained in the sieves with size apertures of 63 μm , 45 μm and 32 μm . This means that the size distribution that is relevant for microscope analysis is $125\mu\text{m} > x \geq 32\mu\text{m}$. It also indicates that the particles can be described as non-colloidal, polydisperse and granules in accordance with the Guide to the Nomenclature of Particle Dispersion Technology for Ceramic Systems. This

is because in any given direction there is a dimension greater than roughly 37 μm and there are several different particle sizes. This means the particles are also not significantly affected by Brownian motion when suspended in water, due to being larger than colloids.

Additionally, any Brownian interactions will be disrupted by hydrodynamic forces for any shear rate value larger than 0.055 sec^{-1} . This is shown by the Peclet number, equation 14, being larger than 10^3 for a suspending medium of water at 20°C. The Stokes number, equation 15, is lower than one for a large range of shear rates for the relevant particle size range of $125\mu\text{m} > x \geq 32\mu\text{m}$ in water at 20°C. This means that the coupling between the olive stone particles and the water will be strong and the particles will move with the flow.

In sieve analysis it is well known that the major source of random error in experimental procedure is sample loss during analysis and blockage within the sieves. To mitigate this issue the experiment was run three times and care was taken to lose as little powder as possible when weighing the samples. The source of systematic error was the sartorius™ digital scale that was used to weigh the powder. It had a precision of three significant figures, so all sample measurements have an error of $\pm 0.005\text{gr}$. This systematic error was carried over when calculating percentages. The relative errors for each measurement were calculated and represented visually in Figure 6 as y-error bars.

Conclusion from Experiment

The size distribution with the highest amount of powder was between $125\mu\text{m} > x \geq 32\mu\text{m}$, with the retained powder in the 250 μm , 125 μm and catching pan being on average lower than 5% of the total powder tested. This indicates that the particles can be described as non-

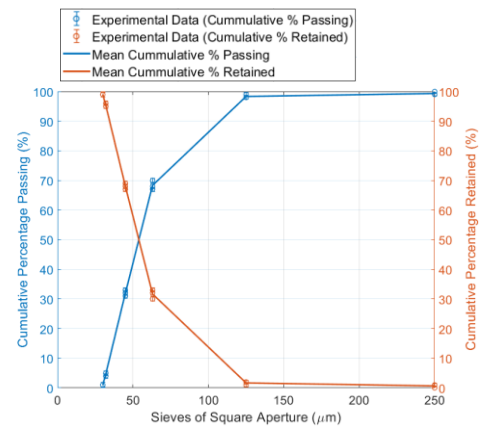


Figure 6: Cumulative Percentage Passing and Retained from Olive Stone Powder

colloidal, polydisperse and granule. This also means that Brownian motion does not significantly affect the particles and due to a low theoretical Stokes number, the coupling between the olive stone particles and water is strong. Finally, it indicates that the size range that will be analysed with a SEM microscope, will be within the $125\mu\text{m} > x \geq 32\mu\text{m}$ range.

4.2. Average Particle Geometry of Olive Stone Powder

Table 4: Results from SEM Study

Size Distribution	N of Particles	Mean l_a (μm)	σ l_a (μm)	Mean l_b (μm)	σ l_b (μm)	Mean r_p	σ r_p
$125\mu\text{m} > X \geq 32\mu\text{m}$	419	65.97	21.30	43.43	13.34	1.52	0.36

For a confidence of 95%, 418 degrees of freedom and a critical t value of ± 1.97 , the confidence interval for all three geometric parameters can be seen in Table 5.

Table 5: Confidence Intervals of Geometric Properties

Geometric Parameter	Mean	Confidence Interval
Major Axis l_a (μm)	65.97	$63.93 < 65.97 < 68.01$
Minor Axis l_b (μm)	43.43	$42.15 < 43.43 < 44.71$
Aspect Ratio r_p	1.52	$1.48 < 1.52 < 1.56$

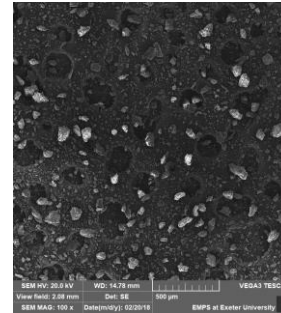


Figure 7: SEM Picture of Olive Stone Powder Particles

Data and Error Analysis

After analysing 419 different particles in the particle size distribution range of $125\mu\text{m} > x \geq 32\mu\text{m}$, a mean aspect ratio of 1.52 was determined with a confidence interval of ± 0.04 . With this value of aspect ratio, the olive stone powder particles can be described as prolate. This means that the local flow around these non-spherical particles will be different than that around spherical ones. Also, as the particles are orientable, their orientation will affect the suspension viscosity. In addition, the degree of interaction between the olive stone particles will be stronger than if they were spherical. Finally, the maximum packing of the olive stone powder particles will be lower than that of spheres because of their prolate aspect ratio.

Conclusion from Experiment

The mean aspect ratio was determined to be 1.52 with a confidence interval of ± 0.04 . This means that the average olive stone powder particle is prolate in shape. As a result, the particles are orientable, interparticle interaction is higher and their random close-packing fraction will be lower than that of spheres (i.e. lower than 0.64).

4.3. Random Close-Packing Fraction of Olive Stone Powder

Table 6: Results from Random Close-Packing Experiment with Olive Stone Powder

Particles: Olive Stone Powder		Aspect Ratio: 1.52 ± 0.04			Density: $1438.1 \text{ Kg/m}^3 \pm 102.9 \text{ Kg/m}^3$						
Container	V_{empty} (m^3)	Test 1			Test 2			Test 3			Mean
		M_p (Kg)	V_p (m^3)	ϕ_m (-)	M_p (Kg)	V_p (m^3)	ϕ_m (-)	M_p (Kg)	V_p (m^3)	ϕ_m (-)	ϕ_m (-)
Box	0.00049	0.33	0.00023	0.47	0.33	0.00023	0.47	0.34	0.00024	0.48	0.47
Sphere	9.05×10^{-4}	0.56	0.00039	0.43	0.57	0.00040	0.44	0.57	0.00040	0.44	0.44

Table 7: Results from Random Close-Packing Experiment with Ball Bearings

Particles: Ball Bearings		Aspect Ratio: 1			Density: $7338 \text{ Kg/m}^3 \pm 1048.2 \text{ Kg/m}^3$						
Container	V_{empty} (m^3)	Test 1			Test 2			Test 3			Mean
		M_p (Kg)	V_p (m^3)	ϕ_m (-)	M_p (Kg)	V_p (m^3)	ϕ_m (-)	M_p (Kg)	V_p (m^3)	ϕ_m (-)	ϕ_m (-)
Box	0.00049	2.55	0.00035	0.71	2.51	0.00034	0.69	2.51	0.00034	0.69	0.70

Data and Error Analysis

From the experiments conducted it was noted that the maximum packing fraction of olive stone powder was lower than that of spherical ball bearings in the container used. This is in line with theory, where prolate particles pack less effectively than spherical particles. The mean experimental random close-packing fraction for olive stone powder was calculated as 0.46 ± 0.07 which will be used as a point of comparison with the suspension viscosity models used in the rheological study. This value is also within the expected theoretical value as prolate particles are known to pack less efficiently than spherical particles^[32]. The mean random close-packing fraction of the ball bearings was calculated to be 0.70 ± 0.1 , which is within the expected value of 0.64 for random packing of spheres.

The systematic error recorded in this experiment was due to the digital scale used to measure the samples. Given that the scale had a precision of two significant figures, all measurements made with it have an error of $\pm 0.05\text{gr}$.

Conclusion from Experiment

The mean value of random close-packing fraction from these experiments for ball bearings was 0.70 ± 0.1 , which is in line with theory of random spherical packing that says the value is 0.64^[32]. The mean value for olive stone packing maximum packing fraction was 0.46 ± 0.07 , which is in line with theory that says prolate particles pack less effectively than spherical particles^[32]. This value was to be compared with those obtained from regression analysis from rheological experiments.

4.4. Rheology of an Olive Stone Suspension

Up Ramp Experiment Data (Assumed 450g/l Particle Concentration)

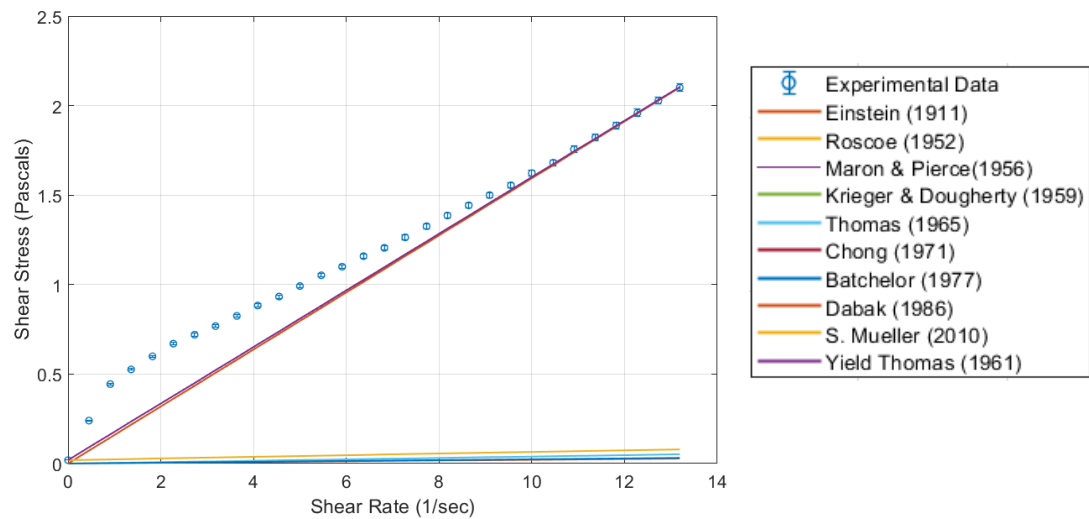


Figure 8: Viscosity Curve Showing Comparison Between Experimental Data and Viscosity Models

Table 8: Percentage Difference Between Viscosity Model and Experimental Data Shear Stress Values

	Einstein	Roscoe	Maron & Pierce	Krieger & Dougherty	Thomas	Chong	Batchelor	Dabak	Mueller	Yield Thomas
Percentage Difference (%)	99.95	5.75	6.03	5.87	98.08	5.64	98.83	5.84	99	4.76

Table 9: Percentage Difference Between Experimental and Predicted Random Close-Packing Fraction

Experimentally Determined Random Close-Packing Fraction: 0.46 ± 0.07						
Model	Roscoe	Maron & Pierce	Krieger & Dougherty	Chong	Dabak	Mueller
Predicted Maximum Packing Fraction from the Model	0.36	0.34	0.34	0.34	0.32	0.57
Percentage Difference from 0.46 (%)	20.00	24.44	24.44	24.44	28.89	26.67
Percentage Difference Considering ± 0.07 Error (%)	7.69	12.82	12.82	12.82	17.95	7.55

Yield Stress Experiment Data

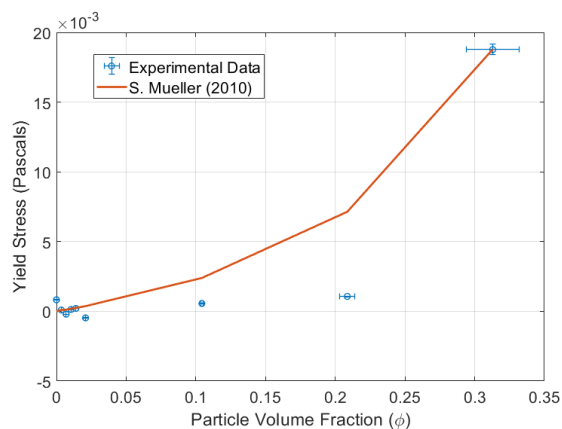


Figure 9: Comparison Between Yield Stress Data and Mueller Model

Table 10: Percentage Difference Between Experimental Data and Mueller Model

	S. Mueller
Percentage Difference (%)	47.21

Time Dependency Experiment Data (Assumed 450g/l Particle Concentration)

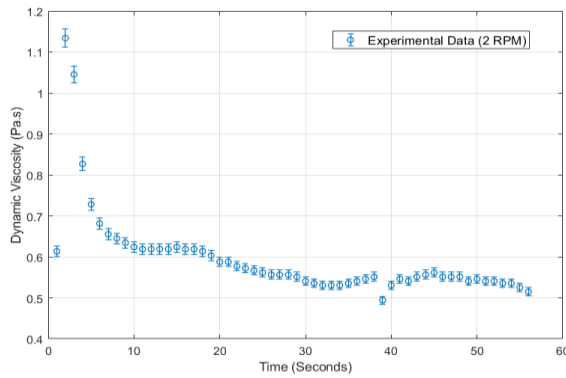


Figure 10: Time Dependency Experimental Data

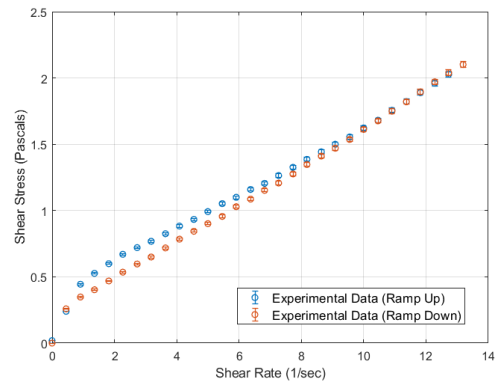


Figure 11: Up and Down Rate Ramp Experimental Data

Data and Error Analysis

Firstly, the data presented is only from an assumed 450g/l sample as the rheometer used had sensitivity issues that will be explained later in the chapter. The analysis that follows is from this single concentrated sample.

From regression analysis, it was established that the Non-Newtonian model proposed by Thomas (Yield Thomas) is the one that most closely predicts the rheological behaviour of the olive stone suspension. This is because the percentage difference between experimental and predicted shear stress is the lowest for Yield Thomas among all the other models as can be seen in Figure 8 and Table 8. However, as stated previously, this model is only applicable in the semi dilute region. This means that the best model to predict the behaviour of an olive stone suspension at a high concentration is the Chong model as seen in equation 20.

Additionally, in Table 9 the values of random close-packing fraction predicted by the viscosity models, except Mueller's, are lower and have an average percentage difference of 25% than that achieved in the separate random close-packing experiment detailed in section 4.3. However, if the experimental error from the random close-packing experiment is considered (i.e. the difference from the closest value from the error interval, for example 0.36 from the Roscoe model to 0.39 of the random close-packing experiment) the average percentage difference drops to 12%, with the Mueller model having the lowest value of 7.55%.

Upon further analysis it was hypothesised that the reason for the above stated difference was due to the concept of concentration profiles. Essentially in settling suspensions the concentration is different throughout the whole container, with the most concentrated section being at the bottom where a sludge bed is formed. Due to the high level of powder in the

450g/l sample, it could be presumed that the sludge bed reached and interfered with the spindle, causing the rheometer to provide readings of a higher unknown concentration. The solution to this issue would have been to use a more viscous Newtonian liquid as a suspending medium but, as will be explained later in the chapter, this was not possible due to budgetary constraints. Interestingly, it was found that if the ϕ_m value of the Mueller model was used as a fitting parameter in regression analysis, instead of a function of aspect ratio, and given a value of 0.33 (with $rp = 1.52$ and $\tau^* = 0.000065$) it provided the best fit to the data as seen in Figure 12.

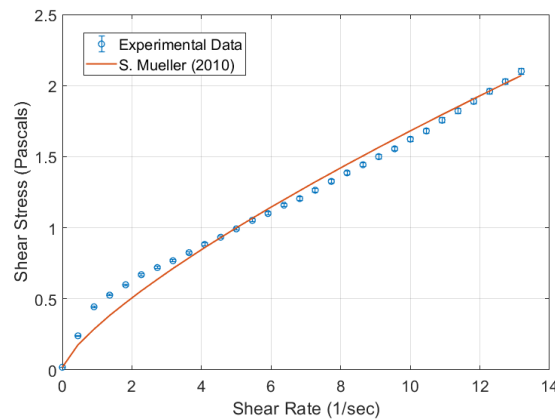


Figure 12: Comparison Between Mueller Viscosity Model and Experimental Data

However, this requires the assumption that the concentration in the whole beaker be 450g/l (i.e. a stable suspension with no settling). Further work would need to be done to validate this assumption.

Despite the above stated assumption, it was decided to extrapolate the rheological behaviour of the olive stone suspension from the concentrated regime to the dilute regime.

Additionally, Figure 9 and Table 10 show that at low particle volume fractions there was no appreciable yield stress, however as the amount of powder in the system increased a yield stress was recorded. This is in line with suspension rheology theory that states, that at high concentrations particles interact as an elastic network, which break up when yield stress is reached [32].

Figure 10 and 11 shows that the dynamic viscosity of the suspension is time dependent. In Figure 11 this is seen with the ramp down shear stress values as they are different to the ones from the up ramp. It can also be seen in Figure 11 that the suspension is shear thinning as the dynamic viscosity decreases as shear rate increases.

The systematic error in the results came from the LVDV-III Ultra as it has an accuracy of ± 1 percent for each specific RPM that is used. The accuracy for each RPM was calculated and is

represented as y-error bars in Figure 8,9,10, 11 and 12. The random error from the experiment stems from uncertainties from sample preparation (i.e. weighing and mixing the powder in the liquid). This was estimated to be ± 3 per cent and is quoted as x-error bars in Figure 9.

It should also be emphasised that the sensitivity of LVDV-III Ultra rheometer, with the spindles that were readily available, was not in the viscosity range of water. This issue can be seen in Figure 9, where a negative yield stress value was reported by the rheometer. After consulting the rheometer manual, it was confirmed that the lowest viscosity reading that could be picked up was 15mPa.s, which is significantly above 1mPa.s, the viscosity of water at 20°C^[81].

The other important factor that was noticed was the rapid settling of the olive stone particles, which occurred at all particle concentrations studied. Several solutions were implemented to overcome this issue: pre-emptive shaking of the suspension, de-flocculants and the introduction of a magnetic stirrer. While the rapid settling could not be overcome in the dilute region, readings were able to be made in the most concentrated sample of 450g/l. But as mentioned before, it was assumed that the concentration throughout the beaker was 450g/l.

It was concluded that measurements in the dilute regime could have been made if one of two actions had been taken: a rheometer attachment had been bought (UL Adapter from Brookfield^[84]), or a viscosity standard liquid had been used as a suspending medium.

However, costing £830 and £130, respectively ^[84], these options were not possible because of the limitations of the £595 student budget and the unpredictable nature of the project (i.e. purchases required to start empirical studies on the sedimentation tanks or buying server space to run simulations).

Taking all these aspects into consideration, the Mueller model was chosen to predict the rheological behaviour of the olive stone suspension and would be the model programmed into the OpenFOAM[®] software. The constants used are $\phi_m = 0.33$, $\tau^* = 0.000065\text{Pa}$, $\mu_0 = 0.0012\text{Pa.s}$ and $r_p = 1.52$. With these values a 3D viscosity curve graph could be plotted as seen in Figure 13:

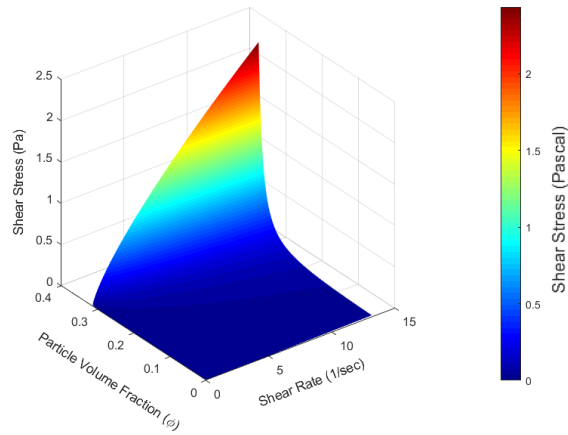


Figure 13: Surface Plot of the Mueller Viscosity Model

Conclusion from Experiment

The olive stone suspension was found to be shear thinning, rapidly settling in water and at high concentrations showed Non-Newtonian behaviour as described by Mueller ^[32].

Extrapolations from higher to lower concentrations helped conclude that the Mueller model provided the best prediction of the rheological behaviour of the olive stone suspension. This is because this model takes several particle related parameters into account which include maximum packing fraction, particle shape and Non-Newtonian behaviour. However, further work will need to be done to completely validate this choice of viscosity model.

4.5. OpenFOAM® CFD Simulations

The Mueller viscosity model was programmed into the OpenFOAM® CFD software and was compared against the default slurry model. The comparison would be between the computational cost of each simulation to reach steady state.

4.5.1. Modified ARMFIELD Rectangular Sedimentation Tank

Computational Cost

From experiments conducted as part of the group project in the Exeter University Fluids lab, the time required to reach a steady state for the modified ARMFIELD rectangular tank was found to be 8 minutes^[67]. Table 11 shows the amount of computational time required for the OpenFOAM® CFD software to reach a simulated time of 8 minutes for the rectangular tank.

Table 11: Computational Cost of the Slurry and Mueller Viscosity Models (Rectangular Tank)

Viscosity Model	Slurry	Mueller
Time Required to Reach Steady State	8.4 Hours	Estimated to be 2.6 Months

The slurry model provided faster simulation speed to get to a steady state when compared to the Mueller model.

It was theorised that the added computational time was due to the solver calculating the three different particle volume fraction dependent parameters of the Mueller model: yield stress, consistency and flow index. In comparison, the Slurry model only has one particle volume fraction dependent term. In conclusion, the Mueller model increased the simulation time by 23,307.91%. It is worth noting that 24 computer cores were used to achieve this simulation speed. If the Non-Newtonian Mueller model is to be made viable, further work would need to be done to either improve the code structure of the Mueller model in OpenFOAM® or use computers with stronger computational power.

4.5.2. Swirl-Flo® Sedimentation Tank

From experiments conducted in the Exeter University Fluids lab, the time required to reach a steady state for the Swirl-Flo® sedimentation tank was found to be 5 minutes^[67]. Table 12 shows the amount of computational time required for the OpenFOAM® CFD software to reach a simulated time of 5 minutes for the Swirl-Flo® tank.

Table 12: Computational Cost of the Slurry and Mueller Viscosity Models (Swirl-Flo®)

Viscosity Model	Slurry	Mueller
Time Required to Reach Steady State	Estimated to be 43.05 Days	Estimated to be 27.6 Years

The slurry model provided faster simulation speed compared to the Mueller model, as seen in the rectangular tank simulation. However, the computational cost increased exponentially due to the complexity of the Swirl-Flo® geometry and mesh quality requirements.

As mentioned before if the Non-Newtonian Mueller model is to be made viable further work would have to be done to increase the efficiency of the code structure. However, due to the speed of the slurry model, it is possible that a quick and accurate simulation result could be achieved with the Newtonian suspension models analysed in section 4.4. These models are those proposed by Roscoe ($\phi_m = 0.36$), Maron & Pierce ($\phi_m = 0.34$), Krieger & Dougherty ($\phi_m = 0.34$ and $B = 5.84$), Chong ($\phi_m = 0.34$) and Dabak ($\phi_m = 0.34$).

However, if the highest possible accuracy is desired then it is recommended that further work is invested in reducing the computational cost of the Non-Newtonian Mueller model.

5. Discussion and Conclusions

5.1. Discussion

The main objective of this individual report was to determine an appropriate viscosity model for an olive stone powder and water suspension, that could be used in the CFD software OpenFOAM® to generate accurate simulation results when compared to empirical experiments of two different sedimentation tanks. The tanks were a Hydrodynamic Vortex Separator or Swirl-Flo® and a modified ARMFIELD rectangular tank.

To accomplish this goal a literature review into the theoretical aspects of suspension viscosity modelling was done. The review in section 2 shows that the most important aspect to consider is the concentration of the suspension, specifically the value of the particle volume fraction as the rheology of the suspension is a function of this value. The review also indicated that characterising the particles of the suspension is important as these characteristics influence aspects of rheological behaviour. Several suspension viscosity models from different authors are also listed, as the field of suspension rheology is iterative and constantly changing.

The first particle characteristic to be determined was the particle size distribution. In this experiment it was found that a standard Sedigraph could not be used to determine the distribution, due to the organic nature of the particles. However, after using a sieve shaker it was found that the range of relevance of the particles was between 125µm and 32µm.

During SEM microscope analysis of the particles within the range of interest, it was found that the resolution of the pictures taken were not good enough to use the image analysis software ImageJ. However, after measuring the particles by hand it was found that the average olive stone particle is prolate in shape with an aspect ratio of 1.52 ± 0.04 . This information was needed for the Mueller viscosity model, equations 25 to 28, and to further characterise the behaviour of the suspension (i.e. greater particle interaction and particle orientation affecting suspension viscosity).

From random close-packing experiments it was found that the random close-packing fraction (i.e. the densest way to pack particles randomly) of the olive stone particles was 0.46 ± 0.07 . This value was used as a point of reference for the rheological studies conducted with the LVDV-III Ultra rotational rheometer, as this value is predicted by suspension viscosity models through regression analysis.

From rheological studies it was found that the olive stone suspension is rapidly settling, shear thinning and showed Non-Newtonian behaviour at high concentrations. Due to issues of rheometer sensitivity and particle settling, measurements could not be made for dilute samples. As suggested in section 4.4 the way to solve this issue would be to purchase either an attachment for the rheometer used or use a viscous standard as the suspending medium. However, from the most concentrated sample of 450 g/l the Mueller^[32] model showed the best fit to the experimental data because it had three particle volume fraction dependent terms that take into consideration the Non-Newtonian behaviour of the suspension at high concentrations. The results from this sample were then extrapolated to the dilute regime of the olive stone suspension. Further work would need to be done to validate this extrapolation.

The Mueller model was then programmed into the OpenFOAM[®] CFD software and compared to the standard Thomas model, equation 19, that is pre-installed in the 2.4.0. version of the software. Due to lack of computational time, the difference in accuracy between the two models could not be studied. However, it was determined that the Mueller model was computationally expensive when compared to the Thomas model, taking 2.6 months to reach 8 simulated minutes compared to 8.4 hours for the modified ARMFELD rectangular tank simulation.

Further work would need to be done to improve the efficiency of the Mueller model for it to become viable. The speed in computational time of the Thomas model was theorized to be due to the simplicity of the model (i.e. only one particle volume fraction dependent term instead of three). It was assumed that the Thomas model, or any of the Newtonian suspension viscosity models described in section 4.4, could potentially be used to achieve quick and accurate simulation results if the unacceptable computational cost of the Non-Newtonian Mueller model cannot be solved.

5.2. Conclusions

- I. The most appropriate suspension viscosity model to predict the rheological behaviour of the olive stone powder suspension is the one proposed by Mueller^[32], as it takes several particle characteristics and Non-Newtonian behaviour into consideration.
- II. When compared to the Thomas model, the Mueller model is currently non-viable for OpenFOAM[®] CFD simulations as 5 simulated minutes for the Swirl-Flo[®] takes an estimated 27.6 years to complete.

5.3. *Further Work*

The use a rheometer that is within the range of sensitivity of water is recommended if the rheological experiments presented want to be repeated with water. If this cannot be done, then the purchase of a viscosity standard that falls within the range of sensitivity of the rheometer is recommended, as this will solve both the sensitivity problem and the rapid settling of particles. It is also recommended to test the validity of the assumptions regarding the stable suspension at 450g/l made in section 4.4, as this was made due to budgetary constraints. Efficiency improvements of the Mueller model for CFD simulations is also recommended, as this was found to be the most accurate in describing the behaviour of the suspension but at the same time was non-viable when used in OpenFOAM®.

6. Project Management

The main strategy used to manage the project was to establish group and individual goals and group cohesion through regularly scheduled group meetings, with and without the project supervisors. A management document was then created at the beginning of the project to set up a working framework and deadlines for key deliverables. It included the budget, group structure breakdown, team member availability, key deliverables, a project workflow and a team Gantt chart. As the project evolved and setbacks caused disruption in the work, the document was updated, and greater detail was introduced. Additionally, all project documents and folders were stored electronically in a cloud server, so all group members could share their ideas and work. This facilitated the group reaching the specified deliverables.

6.1. *Project and Time Management*

Given that the viscosity model is a required parameter for CFD simulations, a placeholder model was given to the CFD team as a way for them to work until an experimentally determined model was introduced. The placeholder viscosity model was the Thomas model which was found to be included as a default model in the OpenFOAM® software. Once the most appropriate viscosity model, the Mueller model, was introduced into OpenFOAM® it was handed over to the simulation team.

6.2. Budget

A budget of £85 per team member was allocated to the entire group, £595 in total, and £171.93 was remaining by the end of the project. The outgoings were high due to the experimental and computational nature of the project. The budget can be seen in Table 13.

Table 13: Group Project Budget

Budget Spent: £423.07 Budget Remaining: £171.93					
Product Purchased	Price	Quantity	Product Purchased	Price	Quantity
20kg Olive Stone Sack	£84.00	2	PVC Pipe Bend	£11.70	1
Petrol for off Campus Trip	£85.00	1	PVC Pipe Reducer	£7.57	1
Seagate 1TB External Hard Drive	£45.99	1	Sphere Containers	£3.54	1
Vortex Stand	£17.95	1	Water Pump and Ball Bearings	£46.48	1
Water Meters	£19.90	1	Filter Papers	£16.94	1

As mentioned previously, a sensitivity attachment to the rheometer and viscosity standard would have cost £830 and £130 respectively. Table 13 does show enough budget remaining to cover the cost of a viscosity standard. However, it was needed early in the project and at that point, due to the experimental and computational nature of the work to be done and the uncertainty of additional required purchases, it was decided that the viscosity standard was too expensive and wouldn't have left sufficient money for last minute purchases (i.e. buying server time to run CFD simulations).

6.3. Sustainability and Health and Safety

Due to the experimental nature of the project, there were immediate health and safety concerns involving the use of olive stone powder. A risk assessment was carried out and from the safety data sheet provided by Goonvean Fibres[®], it was determined that protective gloves, respiratory protection and goggles were to be worn when handling the powder^[7].

The main sustainability concern within the project was the disposal of the olive stone suspension. According to the data sheet from Goonvean Fibres[®], the powder was not soluble in water, but it was expected to be biodegradable. Hence, the powder was to be treated as a controlled waste and disposal was done in accordance with the Exeter City Council.

The broader scope of the project had wider and certainly positive sustainability implications when related to the improvement of wastewater treatment. By determining a viscosity model for an olive stone suspension, a step has been made in the direction of improving the performance of primary wastewater settling tanks.

7. Contribution to Group Functioning

The group project had nine objectives related to the process of creating an experimentally validated CFD model for the behaviour of a sedimentation device, using an olive stone suspension which could potentially then be used to investigate design improvements. To achieve these objectives, the project was separated into seven work packages, all with their own aims to successfully complete the group project. This individual report, together with the work done by A. Wye^[80], satisfies the first and second group objectives specified within the G2 group report. Namely, it describes the determination of an appropriate viscosity model to predict the rheological behaviour of an olive stone suspension and the work done by A. Wye^[80] describes the settling velocity of the powder. Together, these models were used to help achieve the seventh and eight group objectives, since these are key parameters needed to run CFD simulations. Together the two reports mathematically describe the behaviour of the olive stone suspension so that a CFD model, created by R. Bentley^[65], J. Lowe^[85], T. Russell^[66] and T. Scobell^[86], would then be validated by empirical experiments carried out by A. Baker^[67]. Regular face to face meetings kept the group objectives in focus and enabled the creation of a team dynamic that brought about solutions to critical problems that the team was facing, be that regarding CFD, experimental work or report writing.

8. References

- [1] DEFRA, "Waste water treatment in the United Kingdom (2012)," Department for Environment Food and Rural Affairs, London, 2012.
- [2] S. Little, "The Flow Behaviour of Non - Newtonian Sludges," University of Greenwich, London, 1998.
- [3] D. R. Ellis, "The design of storm drainage storage tanks for self cleansing operation," University of Manchester, Manchester, 1991.
- [4] V. R. Stovin and A. J. Saul, "Sedimentation in Storage Tank Structures," *Water Science and Technology*, vol. 29, no. 1 - 2, pp. 363 - 372, 1994.
- [5] W. D. Shepherd, A. P. Saul and J. D. Boxall, "Quantifying the Performance of Storm Tanks," University of Sheffield, Sheffield, 2008.
- [6] Goonvean Fibres, "Product Data Sheet (OSF)," Goonvean Fibres Ltd, St Austell, 2018.
- [7] Goonvean Fibres, "Safety Data Sheet," Goonvean Fibres Ltd, St Austell, 2018.
- [8] R. Bolton and L. Klein, *SEWAGE TREATMENT Basic Principles And Trends*, London: Butterworths & Co, 1961.
- [9] R. Bolton and L. Klein, *SEWAGE TREATMENT Basic Principles And Trends*, London: Butterworths & Co, 1971.
- [10] R. Dick and B. Ewing, "The Rheology of Activated Sludge," *Water Pollution Control Federation*, vol. 39, no. 4, pp. 543-560, 1967.
- [11] D. Novarino, E. Santagata, D. Dalmazzo and M. Zanetti, "Rheological Characterization of Sludge Coming from a Wastewater Treatment Plant," *American Journal of Environmental Sciences*, vol. 6, no. 4, pp. 329-337, 2010.
- [12] G. A. N. Mostoufi, F. Sadeghi, M. Hosseinzadeh, H. Fatourehchi, M. Sarrafzadeh and M. Mehrnia, "COMPARISON BETWEEN DIFFERENT MODELS FOR RHEOLOGICAL CHARACTERIZATION OF ACTIVATED SLUDGE," *Iran. J. Environ. Health. Sci. Eng.*, vol. 8, no. 3, pp. 255-264, 2011.
- [13] Dahl, C. P. (1995). *Numerical Modelling of Flow and Settling in Secondary Settling Tanks*. Aalborg: Hydraulics & Coastal Engineering Laboratory, Department of Civil Engineering, Aalborg University. Series Paper, No. 8
- [14] D. Lakehal, P. Krebs, J. Krijgsman and W. Rodi, "Computing Shear Flow and Sludge Blanket in Secondary Clarifiers," *JOURNAL OF HYDRAULIC ENGINEERING*, pp. 253-262, 1999.
- [15] D. Brennan, "The Numerical Simulation of Two-Phase Flows in Settling Tanks," University of London, London, 2001.
- [16] X. Liu and M. Garcia, "Computational Fluid Dynamics Modeling for the Design of Large Primary Settling Tanks," *JOURNAL OF HYDRAULIC ENGINEERING*, vol. 137, no. 3, pp. 343-355, 2011.
- [17] Versteeg, H. & Malalasekera, W. (2007). *An introduction to computational fluid dynamics: the finite volume method*. Pearson Education Limited. 2nd Edition. England

- [18] G. Hu and T. Kozlowski, "Application of continuous adjoint method to steady-state two-phase flow simulations," *Annals of Nuclear Energy*, vol. 117, no. 2018, pp. 202–212, 2018.
- [19] D. Thomas, "Transport Characteristics of Suspension: VIII. A Note on the Viscosity of Newtonian Suspensions of Uniform Spherical Particles," *JOURNAL OF COLLOID SCIENCE*, vol. 20, pp. 267–277, 1965.
- [20] M. Reiner, "The Deborah Number," *Physics Today*, vol. 17, no. 1, p. 62, 1964.
- [21] Bingham, E.C., "The History of the Society of Rheology from 1924–1944," January, 1944
- [22] Blair, S., *A Survey of General and Applied Rheology*, London: Sir Isaac Pitman & Sons, 1949.
- [23] A. G. Fredrickson, *Principles and Applications of Rheology*, N. J.: Prentice Hall, 1964.
- [24] V. Wazer, J. Lyons, K. Kim and R. Colwell, *Viscosity and Flow Measurement: A Laboratory Handbook of Rheology*, London: Interscience Publishers, 1963.
- [25] K. Walters, *Rheometry*, London: Chapman and Hall, 1975.
- [26] G. W. S. Blair, *Elementary Rheology*, London: Academic Press, 1969.
- [27] J. Douglas, J. Gasiorek and J. Swaffield, *Fluid Mechanics*, London: Prentice Hall, 2001.
- [28] R. L. Mott, *Applied Fluid Mechanics*, New Jersey: Prentice Hall, 2000.
- [29] E. Bingham, "An Investigation of the Laws of Plastic Flow," *US Bureau of Standards Bulletin*, vol. 13, p. 309–353, 1916.
- [30] W. Ostwald, "Ueber die rechnerische Darstellung des Strukturgebietes der Viskosität," *Kolloid-Zeitschrift*, vol. 47, no. 2, p. 176–187, 1929.
- [31] W. Herschel and R. Bulkley, "Konsistenzmessungen von Gummi-Benzollösungen," *Kolloid-Zeitschrift*, vol. 39, no. 4, p. 291–300, 1926.
- [32] S. Mueller, E. Llewellyn and H. Mader, "The rheology of suspensions of solid particles," *Proceedings of the Royal Society A*, vol. 466, no. 2116, pp. 1201–1228, 2010.
- [33] R. Rutgers, "Relative viscosity of suspensions of rigid spheres in Newtonian liquids," *Rheologica Acta*, vol. 2, no. 3, p. 202–210, 1962.
- [34] Rutgers, "Relative viscosity and concentration," *Rheologica Acta*, vol. 2, no. 4, p. 305–348, 1962.
- [35] A. Einstein, "Die Grundlage der allgemeinen Relativitätstheorie," *Annalen der Physik*, vol. 354, no. 7, pp. 591–592, 1916.
- [36] J. Happel, "Viscosity of Suspensions of Uniform Spheres," *Journal of Applied Physics*, vol. 28, no. 11, pp. 1288–1292, 1957.
- [37] H. Brenner, "Rheology of Two-Phase Systems," *Annual Review of Fluid Mechanics*, vol. 2, pp. 137–176, 1970.
- [38] D. Jeffrey and A. Acrivos, "The rheological properties of suspensions of rigid particles," *AIChE Journal*, vol. 22, no. 3, pp. 417–432, 1976.
- [39] W. Pabst, E. Gregorova and C. Bertold, "Particle Shape and Suspension Rheology of Short-Fiber Systems," *Journal of the European Ceramic Society*, vol. 26, no. 1, pp. 149–160, 2006.
- [40] E. Guth and O. Gold, "On the Hydrodynamical Theory of the Viscosity of Suspensions," *Physics Review*, vol. 53, pp. 322–322, 1938.
- [41] V. Vand, "Viscosity of Solutions and Suspensions. I. Theory," *Journal of Physical Chemistry*, vol. 52, no. 2, p. 277–299, 1948.
- [42] R. Manley and S. Mason, "PARTICLE MOTIONS IN SHEARED SUSPENSIONS III: FURTHER OBSERVATIONS ON COLLISIONS OF SPHERES," *Canadian Journal of Chemistry*, vol. 33, no. 5, pp. 763–773, 1955.
- [43] N. Saito, "Concentration Dependence of the Viscosity of High Polymer Solutions. I," *Journal of the Physical Society of Japan*, vol. 5, pp. 4–8, 1950.
- [44] G. Batchelor, "The Effect of Brownian Motion on the Bulk Stress in a Suspension of Spherical Particles," *Journal of Fluid Mechanics*, vol. 83, no. 1, pp. 97–117, 1977.
- [45] A. Donev, I. Cisse, D. Sachs, E. Variano, F. Stillinger, R. Connelly, S. Torquato and C. P., "Improving the Density of Jammed Disordered Packings Using Ellipsoids," *American Association for the Advancement of Science*, vol. 303, no. 5660, pp. 990–993, 2004.
- [46] Jaeger, H. M. and Nagel, S. R. "Physics of Granular States." *American Association for the Advancement of Science*, vol. 255, no. 1524, 1992.
- [47] K. Desmond and E. Weeks, "Influence of Particle Size Distribution on Random Close Packing of Spheres," *Emory University, Atlanta*, 2013.
- [48] I. Krieger and T. Dougherty, "A Mechanism for Non-Newtonian Flow in Suspensions of Rigid Spheres," *Transactions of the Society of Rheology*, vol. 3, pp. 137–152, 1959.
- [49] R. Roscoe, "The viscosity of suspensions of rigid spheres," *British Journal of Applied Physics*, vol. 3, no. 8, p. 267–269, 1952.
- [50] S. Maron and P. Pierce, "Application of ree-eyring generalized flow theory to suspensions of spherical particles," *Journal of Colloid Science*, vol. 11, no. 1, pp. 80–95, 1956.
- [51] J. Chong, E. Christiansen and A. Baer, "Rheology of concentrated suspensions," *Journal of Applied Polymer Science*, vol. 15, no. 8, p. 2007–2021, 1971.
- [52] T. Dabak and O. Yucel, "Shear viscosity behavior of highly concentrated suspensions at low and high shear-rates," *Rheologica Acta*, vol. 25, no. 5, p. 527–533, 1986.
- [53] D. Liu, "Particle packing and rheological property of highly-concentrated ceramic suspensions: ϕ_m determination and viscosity prediction," *Journal of Materials Science*, vol. 35, no. 21, p. 5503–5507, 2000.
- [54] A. Costa, "Viscosity of high crystal content melts: Dependence on solid fraction," *Geophysical Research Letters*, vol. 32, no. 22, 2005.
- [55] F. Boyer, E. Guazzelli and O. Pouliquen, "Unifying Suspension and Granular Rheology," *Physical Review Letters*, vol. 107, 2011.
- [56] Z. Zhu, H. Wang and D. Peng, "Dependence of Sediment Suspension Viscosity on Solid Concentration: A Simple General Equation," *Water*, vol. 9, no. 7, p. 474, 2017.
- [57] T. Papanastasiou, "Flows of Materials with Yield," *Journal of Rheology*, vol. 31, no. 5, pp. 385–404, 1987.
- [58] B. Klein, S. Partridge and J. Laskowski, "Rheology of Unstable Mineral Suspensions," *Coal Preparation*, vol. 8, no. 3/4, pp. 123–134, 1990.
- [59] B. Bbosa, E. DelleCase, M. Volk and E. Ozbayoglu, "Development of a mixer-viscometer for studying rheological behaviour of settling and non-settling slurries," *J Petrol Explor Prod Technol*, vol. 2017, no. 7, p. 511–520, 2017.

- [60] F. Shi and T. Napier-Munn, "Measuring the rheology of slurries using an on-line viscometer," *Int. J. Miner. Process.*, vol. 47, no. 1996, pp. 153-176, 1995.
- [61] S. Kawatra, A. Bakshi and T. Miller Jr., "Rheological characterization of mineral suspensions using a vibrating sphere and a rotational viscometer," *Int. J. Miner. Process*, Vols. 44-45, no. 1996, pp. 155-165, 1996.
- [62] W. Whiten, P. Steffens and J. Hitchins, "An examination of pulp viscosity in tubes at higher shear rates," *Minerals Engineering*, vol. 6, no. 4, pp. 397-404, 1993.
- [63] S. Bokil, "Effect of mechanical blending on the aerobic digestion of the waste activated sludge," *Electronic Theses and Dissertations*, Windsor, 1972.
- [64] P. Monterio, "The influence of the anaerobic digestion process on the sewage sludges rheological behaviour," *Water Science & Technology*, vol. 36, no. 11, pp. 61-67, 1997.
- [65] R. Bentley, "An Investigation into MULES and its Application into Simulating Settling Behaviour in an Armfield Rectangular Settling Tank," *University of Exeter*, Exeter, 2018.
- [66] Russell, "The Use of the Drift Flux Model to Simulate a Hydrodynamic Vortex Separator in OpenFOAM," *University of Exeter*, Exeter, 2018.
- [67] A. Baker, "Validation of Sedimentation Tanks through Empirical Studies," *University of Exeter*, Exeter, 2018.
- [68] J. Cimbala, "Streamlines, Streaklines, Pathlines, and Timelines," 07 January 2015. [Online]. Available: http://www.mne.psu.edu/cimbala/me320web_Spring_2015/Lectures/streamlines_streaklines_etc.htm. [Accessed 17 April 2018].
- [69] A. Jilavenkatesa, S. Dapkunas and L. Lum, *Particle Size Characterization*, Washington: National Institute of Standards and Technology, 2001.
- [70] V. Hackley, *Guide to the Nomenclature of Particle Dispersion Technology for Ceramic Systems*, Washington: National Institute of Standards and Technology, 2000.
- [71] N. Frankel and A. Acrivos, "On the viscosity of a concentrated suspension of solid spheres," *Chemical Engineering Science*, vol. 22, no. 6, pp. 847-853, 1967.
- [72] H. Brenner, "Rheology of a Dilute Suspension of Axisymmetric Brownian Particles," *International Journal of Multiphase Flow*, vol. 1, no. 2, pp. 195-341, 1974.
- [73] J. Stickel and R. Powell, "Fluid Mechanics and Rheology of Dense Suspensions," *Annual Review of Fluid Mechanics*, vol. 37, pp. 129-149, 2005.
- [74] P. Coussot and C. Ancey, "Rheophysical classification of concentrated suspensions and granular pastes," *Physical Review E*, vol. 59, pp. 4445-4457, 1999.
- [75] I. Krieger, "Rheology of Monodisperse Lattices," *Advances in Colloid and Interface Science*, vol. 3, no. 1, pp. 111-132, 1972.
- [76] D. Thomas, "Transport characteristics of suspensions: II. Minimum transport velocity for flocculated suspensions in horizontal pipes," *AIChE Journal*, vol. 7, no. 3, pp. 423-430, 1961.
- [77] British Standards Institution. (2001). BS ISO13317-3:2001: Determination of particle size distribution by gravitational liquid sedimentation methods — Part 3: X-ray gravitational technique. London, England: BSI.
- [78] British Standards Institution. (2012). BS EN 933-1:2012: Tests for geometrical properties of aggregates Part 1: Determination of particle size distribution — Sieving method. London, England: BSI.
- [79] British Standards Institution. (1993). BS 3406-4:1993: Methods for determination of particle size distribution — Part 4: Guide to microscope and image analysis methods. London, England: BSI.
- [80] A. Wye, "Investigation and Development of a Mathematical Model to Describe the Settling Characteristics of Olive Stone Powder," *University of Exeter*, Exeter, 2018.
- [81] BROOKFIELD, "BROOKFIELD DV-III ULTRA PROGRAMMABLE RHEOMETER Operating Instructions Manual No. M/98-211-B0104," BROOKFIELD ENGINEERING LABORATORIES, INC., Middleboro.
- [82] AMETEK Brookfield, "More Solutions to Sticky Problems," Brookfield Engineering Laboratories, 2016.
- [83] OpenCFD Limited, "OpenFOAM The Open Source CFD Toolbox User Guide," 2018.
- [84] BROOKFIELD AMETEK, "LABORATORY VISCOMETERS, TEXTURE ANALYZERS, POWDER FLOW TESTERS INTERNATIONAL DEALERS, DISTRIBUTORS, REPRESENTATIVES". [Online]. Available: <https://www.brookfieldengineering.com/contactus/international-laboratory-rep-list>. [Accessed 17 April 2018]
- [85] J. Lowe, "Investigation into mesh generation using snappyHexMesh for a model Sedimentation Tank and Hydrodynamic Vortex Flow Separator including Volume Of Fluid Simulations," *University of Exeter*, Exeter, 2018.
- [86] T. Scobell, "Investigation into Mesh Generation Techniques Using Pointwise on Primary Sewage Sedimentation Devices," *University of Exeter*, Exeter, 2018.